Pre-normative REsearch for Safe use of Liquid Hydrogen (PRESLHY)

Fuel Cells and Hydrogen Joint Undertaking (FCH JU)

Grant Agreement Number 779613

Deliverable Number:	D4.8
Title:	Experiments and analyses on condensed phases (E4.5)
Authors:	Graham Atkinson
Submitted Date:	15/09/2020
Due Date:	30/06/2020
Report Classification:	CO

FUEL CELLS AND HYDROGEN JOINT UNDERTAKING

Deliverable	
Contractual delivery date	30/06/2020
Actual delivery date	15/09/2020
Deliverable Number	D4.8
Deliverable Name	Experiments and analyses of condensed phases
Internal document ID	EA/20/5
Nature	Report

Approvals			
	Name	Organisation	Date
Author	Graham Atkinson	HSE	24/08/2020
Internal review	Chris Lea	HSE	26/08/2020
External review	Donatella Cirrone	UU	02/10/2020

Disclaimer

Acknowledgments

This project has received funding from the Fuel Cells and Hydrogen 2 Joint Undertaking under the European Union's Horizon 2020 research and innovation programme under grant agreement No 779613. The HSE work programme acknowledges funding from its sponsors Shell, Lloyd's Register Foundation and Equinor and instrumentation provided by NREL and Dräger.

FUEL CELLS AND HYDROGEN
JOINT UNDERTAKING

Publishable summary

This report includes results from experiments and analyses on condensed phase materials and phenomena involved in the release of liquid hydrogen. The objective is to understand the potential risks from explosive events that may arise in ways other than confined or congested gas phase combustion.

Such risks might include condensed phase explosions and Rapid Phase Transitions (RPTs).

The report is divided into three parts:

Part 1: Interaction between pools of accumulated liquid hydrogen and water sprays and jets

This experimental work investigates whether Rapid Phase Transitions and associated pressure effects are to be expected if water from sprinklers or monitors is used to limit the spread of liquid hydrogen.

Part 2: Solids deposited during releases of liquid hydrogen

This is an analytical and modelling study of the condensation and freezing of air when mixed into a liquid hydrogen jet – focussing on the potential for oxygen enrichment. The results are based on a previous experimental study of solid accumulation during liquid hydrogen releases. The report also includes an appendix with a detailed analysis of mass flow results from PRESLHY. These allow a quantitative understanding of the previous experimental work on deposition (where the hydrogen flow rate was uncertain).

Part 3: Behaviour of condensed phases after ignition

The analysis of condensed phase solid deposits and ongoing LH2 flow is extended to include the effect of ignition and the ensuing fire. The purpose of this work is to understand the nature of a violent explosive event that was observed in a previous ignited ground-level jet.

Key words

LH_2, liquid hydrogen, cryogenic, oxygen enrichment, condensed phase explosion, detonation, RPT.

Abbreviations

BP	Boiling point
GH2	Gaseous hydrogen
LFL	Lower flammable limit
LH2	Liquid hydrogen
RH	Relative humidity
RPT	Rapid phase transition
STP	Standard temperature and pressure
UFL	Upper flammable limit

1 Introduction

1.1 Background

This report describes work at the HSE Science and Research Centre on releases of LH_2. The experiments and analyses form part of Work Package E4.5 of the PRESLHY project and focus on the production of condensed phases (solids and liquids) and their interactions with fires and water sprays.

1.2 Objectives

The main objective is to understand the potential risks from explosive events that may arise in ways other than confined or congested gas phase combustion. Such risks might include Rapid Phase Transitions and condensed phase explosions.

To meet this objective a number of different types of work were carried out and the report is divided into three separate parts:

Part 1: Interaction between accumulated liquid hydrogen and water sprays and jets

This preliminary experimental work investigates whether rapid phase transitions and associated pressure effects are to be expected if water from sprinklers or monitors is used to limit the spread of liquid hydrogen.

Part 2: Solids deposition during releases of liquid hydrogen

This is an analytical and modelling study of the condensation and freezing of air when mixed into a liquid hydrogen jet – focussing on the potential for oxygen enrichment. The results are based on a previous HSE experimental study of solid accumulation. The report also includes an appendix with a detailed analysis of mass flow results from PRESLHY E3.5. These flow rate data allow a better quantitative understanding of the previous experimental work on deposition (where the hydrogen flow rate was uncertain).

Part 3: Post-ignition behaviour of solid phase materials

The analysis of condensed phase deposits is then extended to include the effect of ignition, melting and vaporisation. The purpose of this work is to understand the nature of a violent explosive event that was observed in a previous ignited ground level jet.

2 Part 1: Interaction between liquid hydrogen and water sprays

2.1 Experimental methods

The experiments were conducted using the LH_2 release facility, which was located on a 32 m diameter concrete pad at the Frith Valley site at the HSE Science and Research Centre in Buxton.

The experimental set up is illustrated in Figure 1.

Liquid hydrogen from a tanker with a vapour pressure of around 200 mbarg (~22K,-251°C) entered via a vacuum insulated 1" hose (A). All fittings up to the open end of the pipe were foam insulated to minimise the exit vapour fraction and maximise the rate of liquid accumulation. The tanker ullage was at the liquid vapour pressure and the total head (including gravity) was less than 300 mbar. Flow was controlled using a pneumatic valve (B) – this was covered in plastic to protect it from water damage in cryogenic conditions. The flow of liquid discharged into an open channel cut in a foam block (C). Liquid from this channel ran into an 800 x 800 mm x 100 mm deep tray constructed from foam and lined with aluminium foil (D).

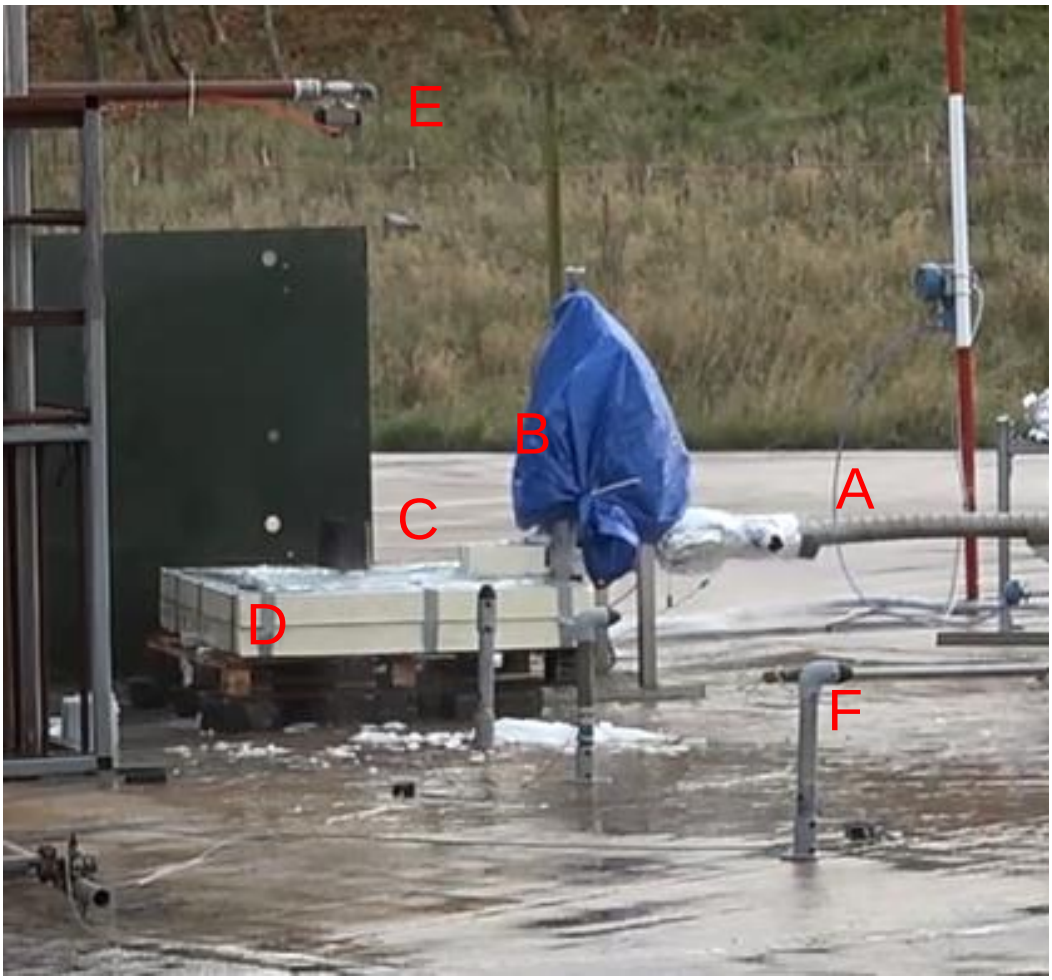

Figure 1: Experimental set up

Water was delivered using two standard ½" sprinkler heads or an open 1" pipe at an elevation of 1500 mm above the pool of accumulated liquid hydrogen (E). Water flow was controlled using a pneumatic valve. Water pressure at the openings was around 3 bar.

Two stages of water application from sprinklers are illustrated in Figure 2 and 3. Figure 2 shows the developing water spray around the two heads immediately after activation. Figure 3 shows the fully developed spray. The final traces of mist caused by vaporisation of liquid hydrogen are visible just above the foam tray but most of the white cloud is the water spray.

Figure 4 shows the water jet delivered by the open nozzle. This impacted around the centre of the pool tray.

Figure 2: Water issuing from sprinklers immediately after activation

Figure 3: Fully developed water spray from sprinklers

Figure 4: Water jet application into the centre of the tray

The water application rate was measured by timing the rate of accumulation in the empty pool tray. In the case of sprinklers the delivered density was around 9 mm/min.

It took 13 seconds for the water jet to fill the pool to a level of 100 mm. Averaged across the pool surface this corresponds to 460 mm/min.

Kulite pressure transducers (marked F in Figure 1) were used to record potential shocks from rapid phase transitions.

Vertical arrays of T-type thermocouples (spaced at 20 mm intervals) were used to monitor the level of the deepening pool of liquid hydrogen in the tray. Data logging with National Instruments chassis and logging card was at a rate of 1 Hz.

The tests were recorded with conventional and high speed video. Weather data was collected covering the test periods.

2.2 Test programme

Both sprinkler and jet tests were carried out on the afternoon of 30th October 2019. The temperature was 7 °C and average wind speed around 4 m/s, relative humidity was around 50%.

The pool took about 600 seconds to accumulate to a depth of 700 mm. Dense clouds of condensation surrounded the filling area throughout, suggesting that there was a large rate of loss throughout. Despite best efforts to minimise driving pressure and heat input, the outlet velocities were quite high and most of the liquid hydrogen did not run in the foam channel but sprayed out, impacting the rear wall of the pool.

When a sufficient depth of liquid hydrogen had accumulated the hydrogen supply was stopped and water supply started (roughly 700 s).

2.3 Results

2.3.1 *Sprinkler test*

Temperatures in the thermocouple rake[1] during the sprinkler test are shown in Figure 5.

[1] These stable low temperatures recorded correspond to liquid hydrogen. Difficulties in calibration at these low temperatures account for the difference from the true boiling point of hydrogen. This is discussed in detail in the PRESLHY report on WP 3.6.

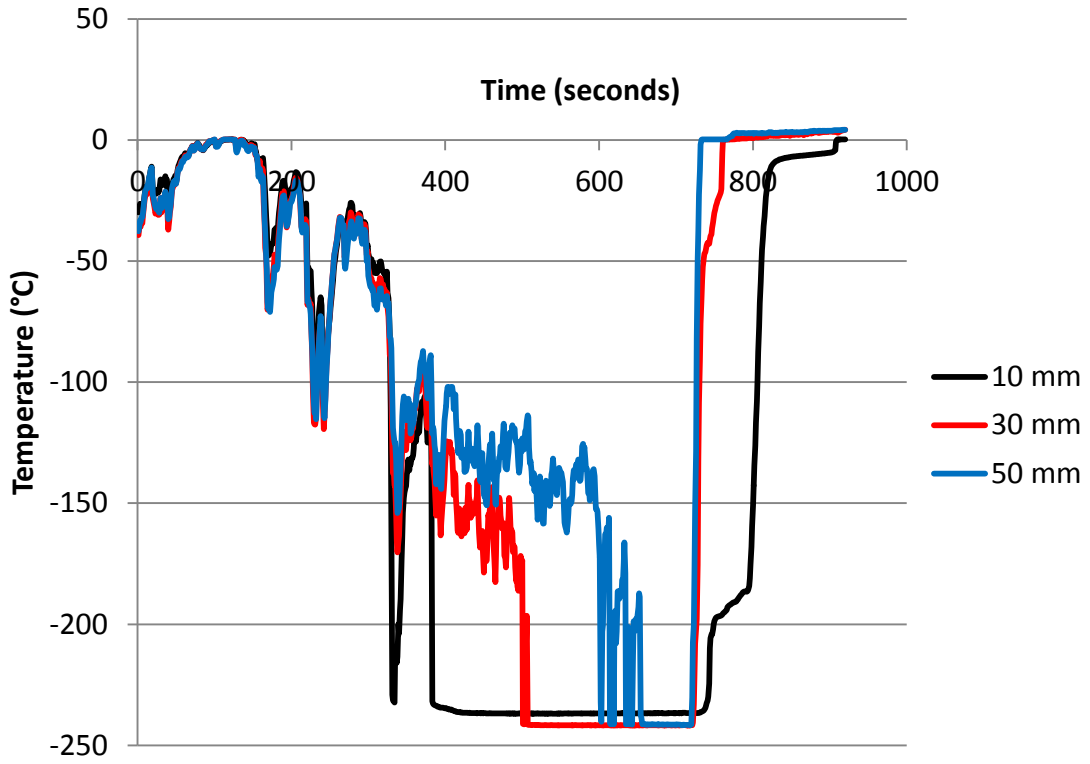

Figure 5: Pool thermocouples during the sprinkler test (different distances from pool base)

Most of the vapour production was complete within about 30 seconds (Figure 6 a-d).

There was no sign of rapid phase transition. No significant pressures were recorded. After the test, the pool tray was about half-full of ice. Water droplets had presumably frozen as they sunk through the cryogenic liquid.

Temperature records suggest there was an accumulation of condensed air at the bottom of the tray.

Figure 6a: Vapour production after 5 seconds of spray impingement

Figure 6b: Vapour production after 10 seconds of spray impingement

Figure 6c: Vapour production after 20 seconds of spray impingement

Figure 6d: Vapour production after 30 seconds of spray impingement

2.3.2 *Water jet test*

Temperatures in the thermocouple rake during the water jet test are shown in Figure 7.

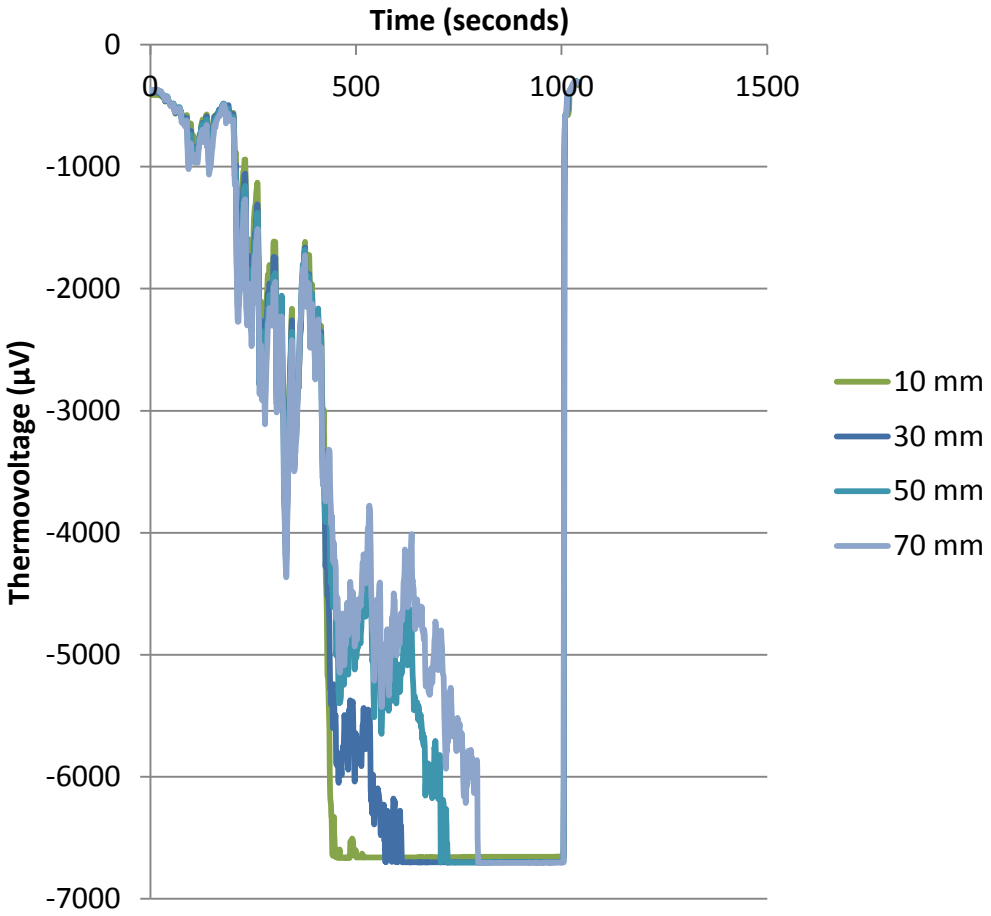

Figure 7: Pool thermocouples during the water jet test

Most of the vapour production was complete within a few seconds (Figure 8 a-c).

There was no sign of rapid phase transition. No significant pressures were recorded. After the test there were no signs of ice in the pool tray. Presumably water displaced the liquid hydrogen so rapidly that there was no time for it to freeze. The displacement was probably a combination of rapid in situ vaporisation and physical displacement as a result of water flow and rapid vapour production.

Figure 8a: Vapour production after 1 second of jet impingement

Figure 8b: Vapour production after 3 seconds of jet impingement

Figure 8c: Vapour production after 10 seconds of jet impingement

2.4 Conclusion: Risks from RPT during emergency application of water

The tests showed that contact between water and liquid hydrogen will not necessarily cause a RPT – even if the water is discharged directly downwards as a jet into a pool of liquid hydrogen. However the factors leading to the occurrence of RPTs are not well understood and the results do not guarantee that energetic events would not occur in other circumstances.

The work gives preliminary reassurance that sprinklers and monitors (water jets) can be used to control the flow or accumulation of liquid hydrogen without risking the occurrence of RPT. Obviously the rate of vaporisation is enhanced and if ignited there could be a larger initial fireball.

3 Part 2: Solid phase formation in liquid hydrogen releases

HSE research reports RR986 and RR987 describe experiments on unignited and ignited low pressure (1 bar) jets of liquid hydrogen. Further details of the discharge arrangements for those experiments is given in Appendix 1.

Cases where the jet runs horizontally, close to the ground, were of particular interest. This is because a substantial solid deposit accumulated away from the outlet and when ignited (Test 6 RR987) there was a significant secondary explosion, about 3.5 seconds after the initial flash fire. In this particular test, the wind speed during accumulation was approximately 2 m/s in a direction roughly parallel to the jet.

The morphology of the accumulated solid was clearly recorded but its composition and density were not measured so it is not possible to confirm many of the results of the analysis that follows. Many of the conclusions, therefore, remain speculative at this stage but may be useful in guiding future work.

Following the secondary explosion, the fireball expanded in less than 100 ms to a volume approximating to a hemisphere of diameter 8 m. As it lifted off, this fireball appeared to be at least as large as that associated with the initial flash fire following ignition (Figure 9). Higher radiant intensities were also observed.

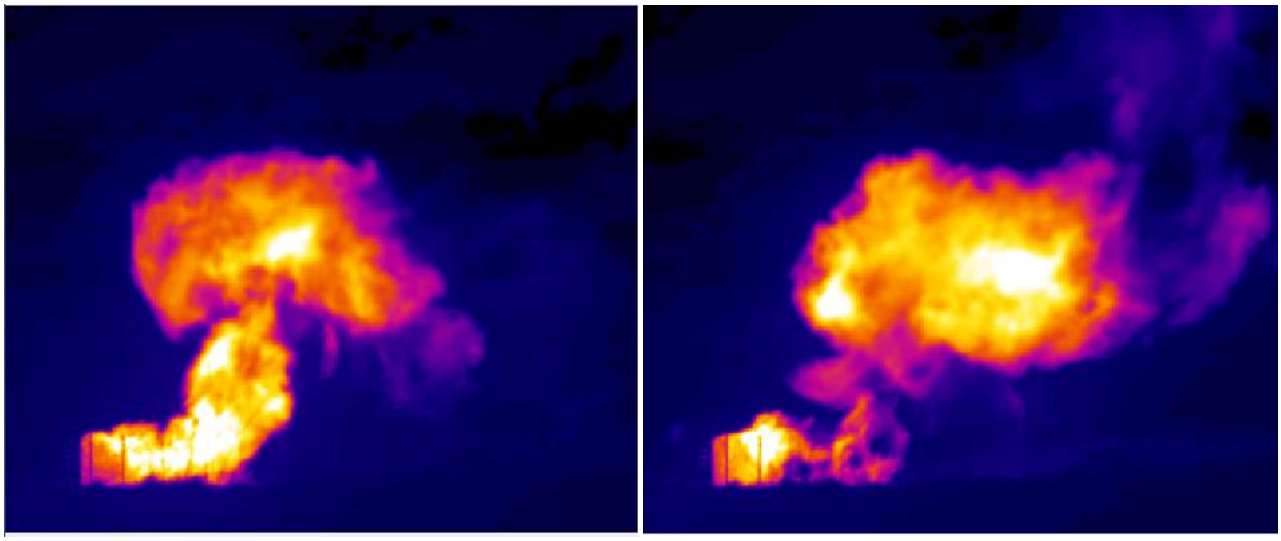

Figure 9: Comparison between fireball caused by the initial flash fire (left) and the secondary explosion (right)

The approximate hydrogen consumption necessary to fuel such a fireball can be estimated from its volume.

Volume of combustion products = 134 m^3

Volume of stoichiometric STP hydrogen required = 19 m^3 (Assuming an expansion ratio of 7 for such a mixture) In this case the initial state of the fuel and oxidant may not have been gaseous and certainly not at STP but the final state in the fireball would have been fairly similar.

Volume of hydrogen required = 0.29 x 19 = 5.5 m^3

Mass of hydrogen required = 5.5 x .085 = 460 g

Approximately 3.7 kg of oxygen would also have been required. This would have corresponded to about 18 kg of air or a smaller quantity of oxygen–enriched material (e.g. 4.8 kg of material at the O_2-N_2 eutectic composition – 77% mol/mol O_2 – see Figure 24). Some of the oxidant may have come from rapid afterburning at the edge of a hydrogen-rich cloud in surrounding air. However, the time scale of expansion seems too short for this to have been the dominant source of oxygen.

Repeat tests did not reproduce the secondary explosion. Probably this means that wind conditions (which varied in subsequent tests) are important in allowing the accumulation of solid air with the necessary degree of oxygen enrichment.

This section discusses the formation of solid deposits during the release of liquid hydrogen with the objective of determining how the quantity, composition and temperature of these deposits vary with conditions of the release. In the next section, the behaviour of solids after ignition is examined to determine in which ways they might have contributed to the secondary explosion described in RR987.

3.1 Observations of deposition of solids

Figure 9 shows an unignited, ground-level, horizontal liquid hydrogen jet in progress. In this case the mass flow rate was about 135 g/s (See Appendix) through a 1" internal diameter open pipe. This corresponds to an equivalent liquid volume flow rate of 1.9 litres/second. The nominal volume flow of gaseous hydrogen (at its BP and pressure 1000 mbar) would have been about 0.115 m^3/s.

Vaporisation in the final section of the delivery system would have reduced the density at the outlet. The extent of vaporisation is not known but comparison with the amount of uninsulated pipe in PRESLHY suggests the density would have been somewhat less than 20 kg/m^3. Probably the density would have been in the range 10-20 kg/m^3 in which case the total volume flow rate at the nozzle would have been about 6.5 – 13 litres/second, which corresponds to a nozzle velocity of 13-26 m/s.

Figure 9: Ground level, horizontal liquid hydrogen jet in progress

The nozzle was directed slightly downwards so that the stream of liquid and gas would have impacted the ground. Most of the liquid flow would initially have been along the ground but there would have been some gas and droplets above.

Figure 9 shows the mixing of air into the co-flow of cold hydrogen gas surrounding the central ground flow of liquid hydrogen. Formation of condensed phases of air (presumably liquid and solid) is visible in the mixing zone. These droplets and crystals would have been carried along in the flow of hydrogen gas but the speed of this gas flow would have slackened rapidly as the mass fraction of air increased. Droplets and crystals would have been deposited in areas where the flow fell to a sufficiently low level.

Hydrogen vapour at its boiling point has a density fairly close to that of air, however entrainment of air certainly reduces the velocity of the flow and may increase the density. At some stage, it is possible that additional entrainment could be significantly restricted by buoyancy effects. This possibility is discussed further below.

Figures 10 and 11 show the solids that had accumulated after 7 minutes.

Figure 10: Solid deposits accumulated after 7 minutes

Figure 11: Solid deposits accumulated after 7 minutes (close-up)

The majority of the solid is at a range of about 2.7 to 3.5 m from the nozzle extending to a width of about 0.5 m. There is a much smaller amount of solid material deposited on one edge of the jet. The asymmetry in deposition was presumably caused by a crosswind (entrained air imparts transverse momentum to the flow of cold hydrogen and condensed air).

Figure 12 shows the state of the deposit 20 seconds after the image in Figure 11. This image shows more clearly the relationship between the track of the hydrogen jet and the areas of deposition. It is clear that (in this case) when air was entrained by the hydrogen jet in a cross-flow, the mixture generally retained sufficient momentum in the direction of the wind to carry it away from the jet axis before deposition occurred.

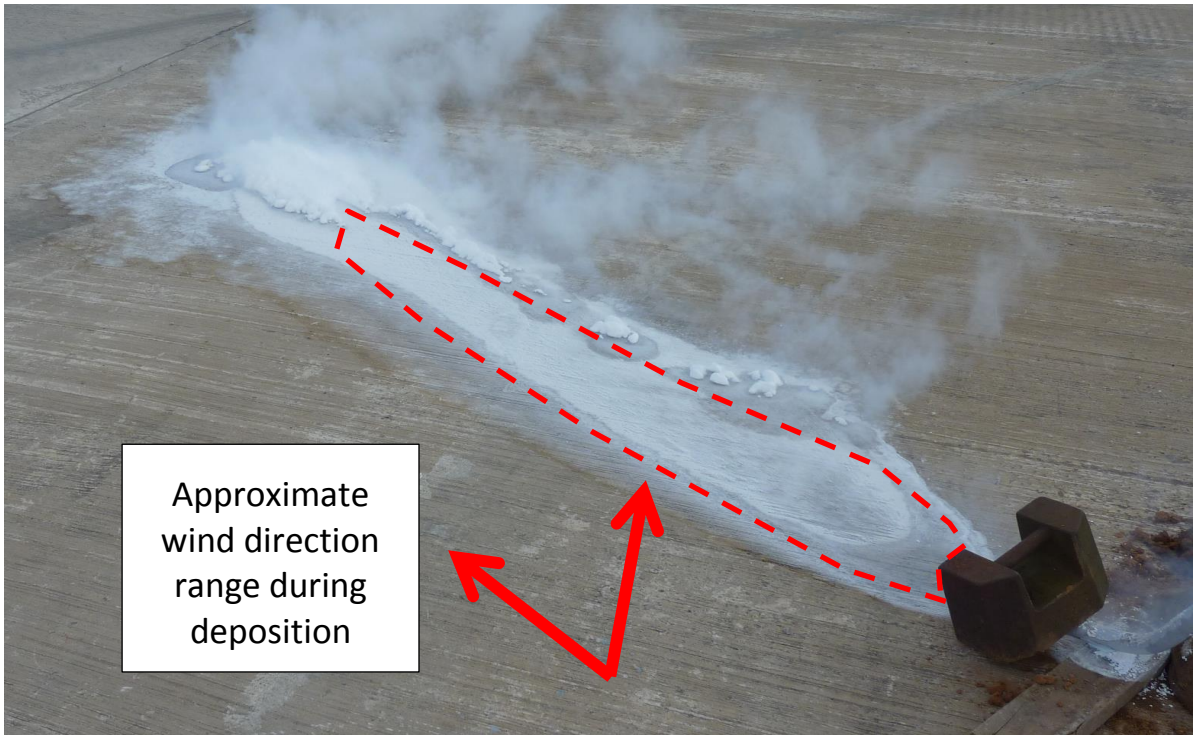

Figure 12: Melting deposits (20 seconds after Figure 10). The approximate track of the hydrogen flow is marked

The total volume of the solid deposit appears to have been around 40 litres (500 x 800 x 100 mm), which would amount to approximately 36 kg - assuming the deposit had the same density as nitrogen frost (https://en.wikipedia.org/wiki/Solid_nitrogen).

In the unignited test shown in Figures 9 to 12 (for which the ground was somewhat pre-cooled by previous releases) approximately 36 kg of solid deposit accumulated in 7 minutes (420 seconds).

The ignited Test 6 involved accumulation for 260 seconds (the ground was also somewhat pre-cooled by previous releases). The time taken before the ground was sufficiently cold to allow the solid to form efficiently would have been a larger fraction of the total duration. This effect is examined in 3.3.2 and the conclusion is that (assuming a similar level of pre-cooling) the amount of solid deposit in Test 6 would have been approximately 260/420x36x0.78 = 17 kg. There are a number of substantial assumptions in this assessment and the uncertainty in the result is probably +/- 5 kg.

It would be particularly useful to know the density of solid deposits.

The overall width of the solid deposit is of interest as it gives some indication of the flow speed of the hydrogen as this point. It is shown later that solid only forms for hydrogen/air molar ratios of about 10 and temperatures of about 50 K. The volume flow of gas is therefore dominated by hydrogen and amounts to a maximum of about 0.22 m^3/s (based on the mass release rate and a maximum temperature of 50 K). If the half width and height of the flow surrounding the solid is >0.25 m, the cross sectional area of the flow must be at least 0.1 m^2. This means the flow speed of hydrogen must have been less than 2.2 m/s.

3.2 Condensation of air

Calculations (by the author) in this section have been made on the assumption that the components of the nitrogen-oxygen-hydrogen system behave ideally i.e. the equilibrium vapour pressure of air components is determined only by the mole fraction in the liquid phase. It has also been assumed for simplicity that air contains only nitrogen and air; minor components apart from water (e.g. argon) are counted as nitrogen. This is not likely to make a significant difference to the assessment of the properties of the solid deposit compared with uncertainties in the statistics of entrainment, i.e. the range of air to hydrogen ratios.

Figure 13 a-d shows the results of analysis of the equilibrium state for the adiabatic mixing of **liquid** hydrogen (at the boiling point) with air at 288 K (RH 0%).

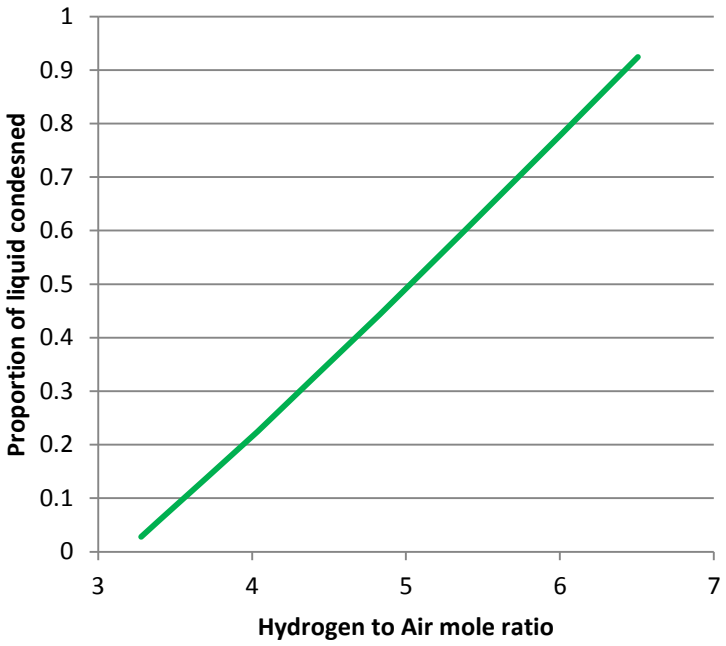

*Figure 13a: Equilibrium state of **liquid** hydrogen and air mixed in different proportions - Molar proportion of air condensed*

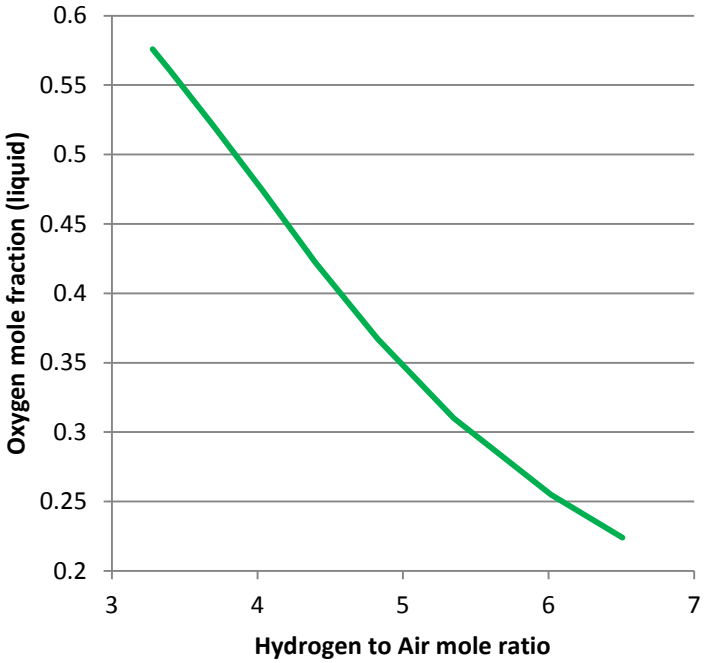

*Figure 13b: Equilibrium state of **liquid** hydrogen and air mixed in different proportions - Mole fraction of oxygen in the condensed liquid*

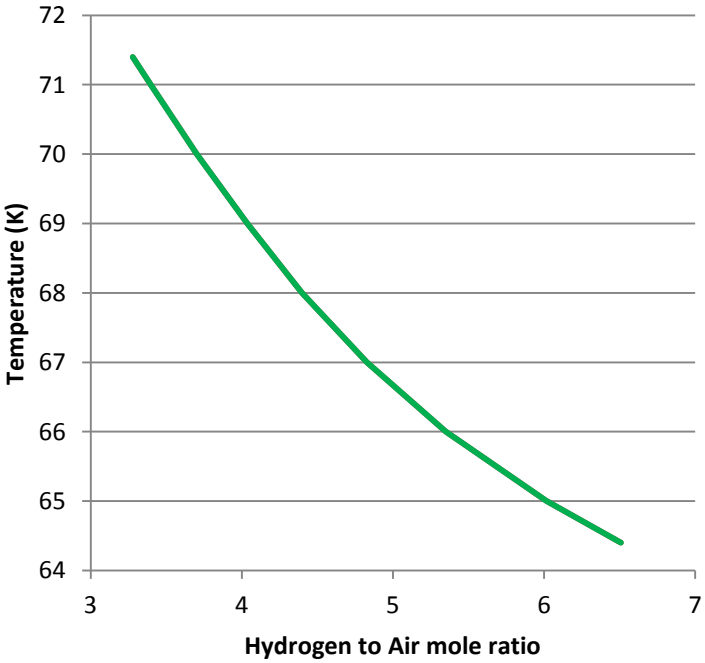

*Figure 13c: Equilibrium state of **liquid** hydrogen and air mixed in different proportions - Temperature*

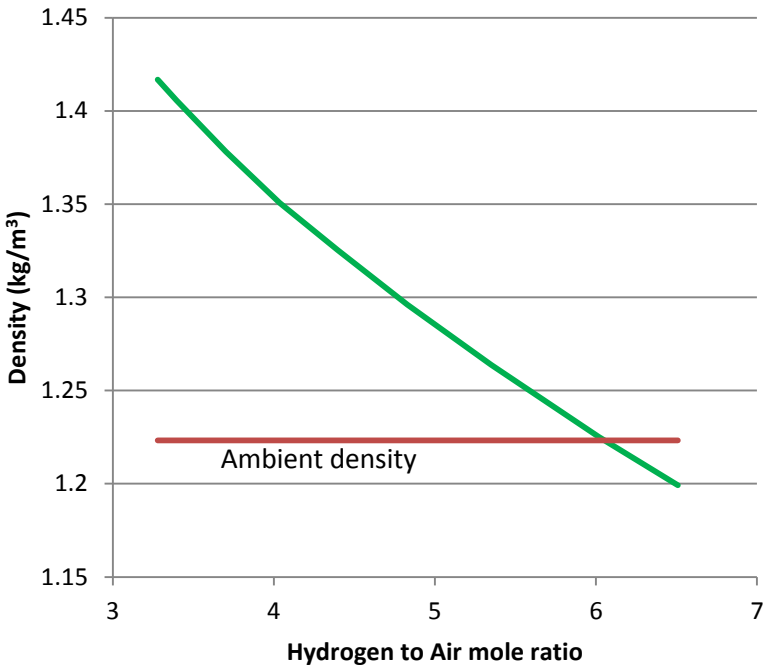

*Figure 13d: Equilibrium state of **liquid** hydrogen and air mixed in different proportions - Mixture density – all phases*

It is also useful to determine the results of mixing of gaseous hydrogen (initially at the boiling point) with air in various proportions. In this case larger hydrogen/air ratios are required to produce condensation of air than in Figure 13 a-d because the air does not have to vaporise the hydrogen. A given quantity of hydrogen can only chill a smaller amount of air to the boiling point

Figure 14 a-d shows equivalent results for the mixing of gaseous hydrogen (at the BP) with air.

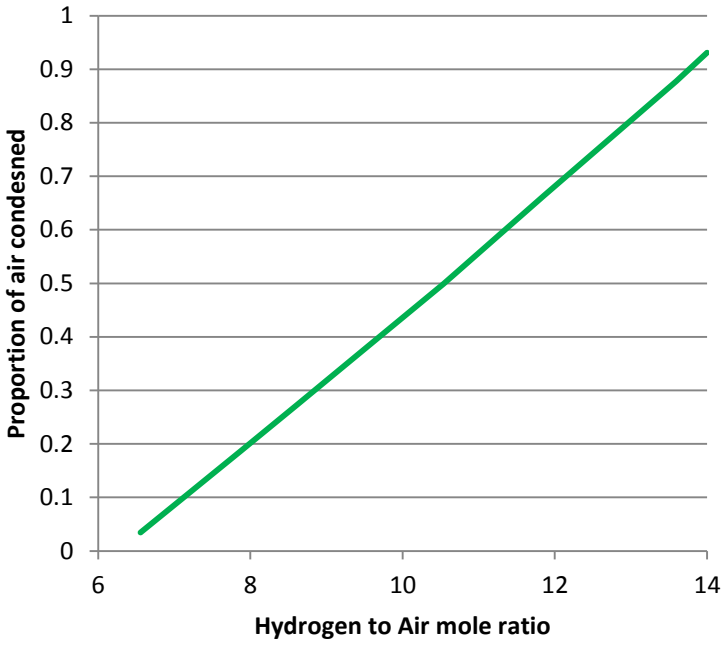

*Figure 14a: Equilibrium state of **gaseous** hydrogen and air mixed in different proportions - Molar proportion of air condensed*

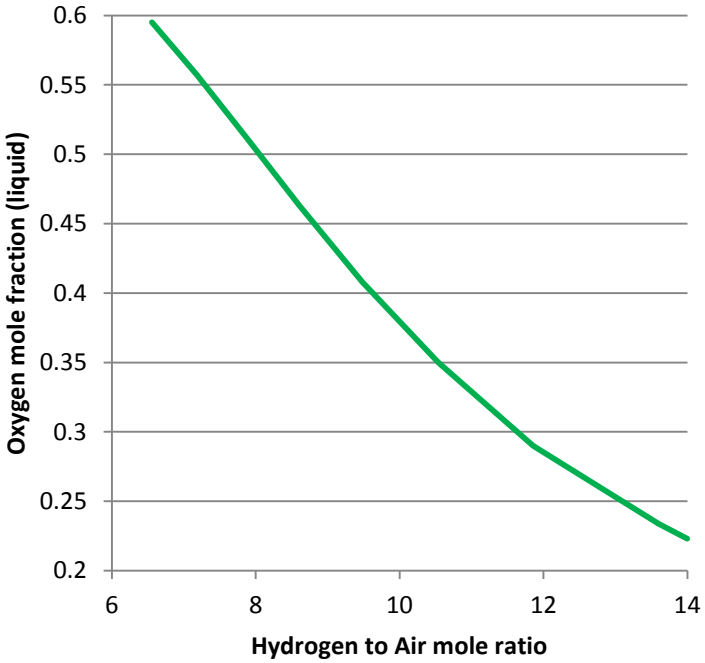

*Figure 14b: Equilibrium state of **gaseous** hydrogen and air mixed in different proportions - Mole fraction of oxygen in the condensed liquid*

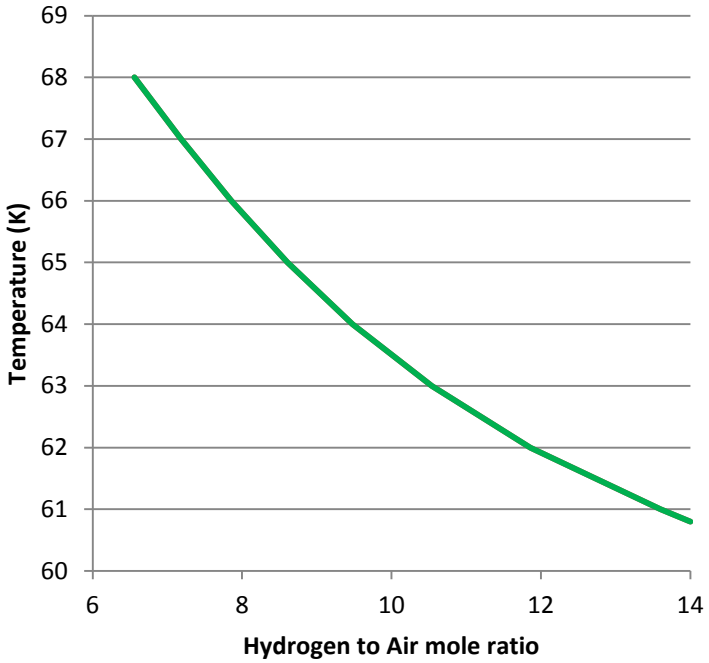

*Figure 14c: Equilibrium state of **gaseous** hydrogen and air mixed in different proportions - Temperature*

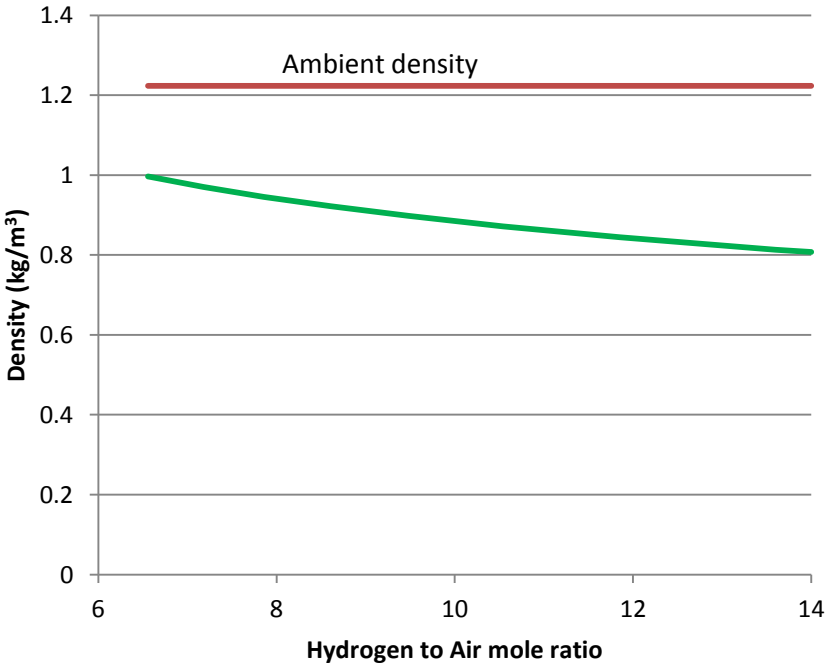

*Figure 14d: Equilibrium state of **gaseous** hydrogen and air mixed in different proportions - Mixture density –all phases*

Air (initially at 288 K) is fully condensed if the hydrogen to air (molar) ratio exceeds about 14. This corresponds to temperatures less than about 61 K. Liquid fully condensed

by contact with such a large amount of hydrogen clearly has the same composition as air, i.e. there is no oxygen enrichment.

If more air is present, the proportion of air as a condensed liquid phase falls. If the hydrogen to air ratio is about 6 or less there is no condensation of air (it all remains in the gas phase). For hydrogen to air ratios between 6 and 14 there is a varying degree of oxygen enrichment. The first liquid formed as more hydrogen is mixed in with air has an oxygen mole fraction of around 60% and this is at a temperature of around 69 K.

Even for dry air the density of the hydrogen gas/air mixtures (with varying degrees of condensation) is well below that of ambient air, i.e. they are buoyant.

All of the results in Figure 14 a-d vary slightly if the air is moist, for example for at 100% relative humidity (288 K) the limiting molar ratio at which condensation is complete increases to around 15.4.

3.3 Non-equilibrium conditions

The whole flow is nowhere near equilibrium at any stage during the deposition process. Warmer, air-rich gas flows above the LH2 and there is only a close approach to equilibrium conditions where there is close contact between air and LH2.

Figure 15 shows how the density of a mixture of dry air (288K) and LH2 (at BP) varies as the proportion of hydrogen increases. The density of the gas phase portion of the mixture is also shown. The mole ratios shown corresponds to the range over which condensation of air occurs (see Figure 13). Note in this case heat is transferred from the air to both vaporise the LH2 and to raise the resulting GH2 to the final temperature (which is in the range roughly 64 -71 K for the molar ratios shown).

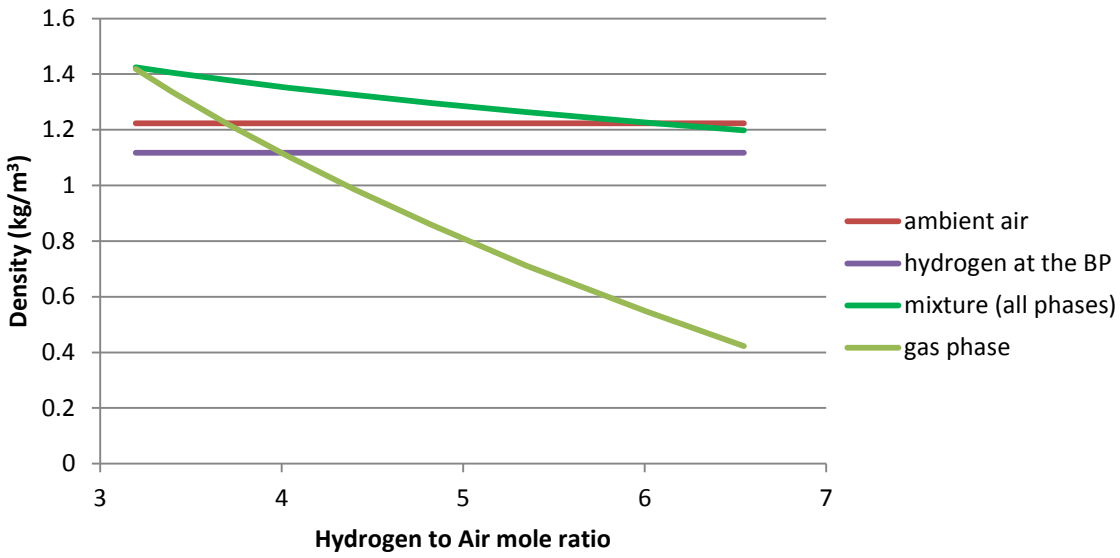

Figure 15: Density of a mixture of air (initially at 288K) and LH2 (at BP)

Up to a GH2/air ratio of about 3 the air/GH2 mixture is purely gaseous and denser than fresh GH2 released at the surface. This density difference will promote mixing of GH2

released from the pool with air in the parcel. Heat transfer to the pool surface and release of additional hydrogen will continue rapidly.

Condensation of air starts at H/air ratios just over 3 and the density of the complete mixture remains above that of fresh hydrogen even for high GH2/air ratios. However, if there is deposition of the oxygen-rich condensed phase as it forms, the density of the remaining gas falls rapidly. Above a H/air ratio of 4 the residual gas becomes lighter than any hydrogen given off at the surface and it will not easily displace hydrogen from the surface to allow heat transfer to progress. Figure 13b shows that at this H/air ratio the level of oxygen enrichment is around 50% mole/mole.

On the other hand, the nitrogen-rich gaseous residue is much lighter than overlying gas that has not begun to condense. Mixing with this overlying gas is enhanced, bringing fresh oxygen rich gas down to the interface.

This view of the entrainment process is shown schematically in Figure 16.

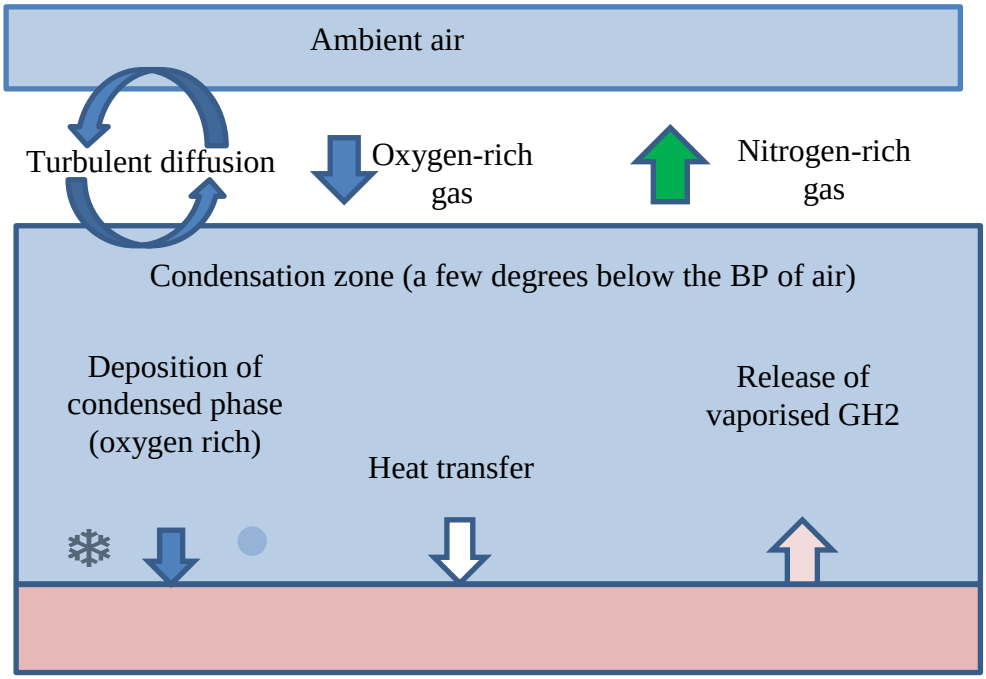

Figure 16: Schematic showing mixing and deposition process

In conditions of slow mixing, where deposition of the condensed phase has time to occur - the following sequence seems credible as a parcel of air moves down closer to the interface with LH2:

1. Air mixes with increasing amounts of cold GH2 until it is cooled to the initial boiling point of air;

2. A liquid phase forms that is rich in oxygen (about 60% mole/mole);

3. The density begins to fall;

4. More hydrogen is entrained and more liquid is formed (with a somewhat lower oxygen content) – the density continues to fall;

5. Droplets of condensed air (~50% O_2 mole/mole) settle out of the mixture producing a more substantial drop in density;

6. The residual gas density becomes so low that further mixing of hydrogen from below is suppressed. Mixing with overlying air is enhanced, bringing mixtures with higher oxygen concentrations down to the interface;

7. There is deposition of oxygen rich droplets/crystals at the LH2 surface;

8. Heat transfer to sustain hydrogen vaporisation comes from thermal contact between gas (in the condensation zone) and the LH2 surface – as well as heat associated with deposition of (warmer) solids;

9. The temperature in the condensation zone does not fall far below the initial BP of air (where full condensation of air without oxygen enrichment would occur) because this would involve:

(i) A big drop in density;

(ii) Suppression of mixing with evolved hydrogen; and

(iii) Reduction of heat transfer to LH2 - removing the driver for low temperatures.

Condensation is constrained to occur in conditions where oxygen enrichment of the condensed phase is possible.

For this to work as a mechanism for oxygen enrichment of deposits, the gas immediately above the liquid must not be disturbed (at least not on the time scale necessary for deposition of condensed material on the surface).

These arguments suggest that relatively high levels of oxygen in deposited material may be associated with relatively slow mixing, i.e. low relative velocities between the GH2/LH2 and overlying air. The composition of deposited material consequently depends on wind and liquid release conditions. In a spill into a tray, the surface of accumulated LH2/GH2 is not moving on average. High levels of oxygen enrichment might be expected in the lowest wind speeds.

In an unconfined ground level jet such as that in RR987, the LH2/GH2 will be moving away from the liquid outlet at different speeds and distances from the outlet. Probably the highest level of overall oxygen enrichment would occur with a gentle wind in the direction of the jet and in the parts of the ground flow where the speed is low (minimising the relative speed of LH2 and air). Potentially different parts of the accumulated deposit might have different compositions depending on the flow conditions where they were formed.

3.4 Composition and temperature of solids

The heat of vaporisation of molecular hydrogen (H_2) is approximately 0.9 kJ/mol. The enthalpy change of air (initially at 288 K) to solid at the boiling point of hydrogen (21 K) is approximately 15.4 kJ/mol. Therefore, vaporisation of at least 17 moles of liquid hydrogen is required to condense, solidify and cool 1 mole of air to the boiling point of hydrogen. Mixed solid air and liquid hydrogen can therefore only occur together stably in locations where hydrogen is in very large molar excess.

Table 1 shows a summary of the equilibrium phase composition of mixtures of liquid hydrogen and air at 288 K.

Table 1: Phase composition of mixtures of liquid hydrogen and dry air at 288 K

Temperature range	**Phase**	**Hydrogen to air (molar) ratio**
21 K	Liquid hydrogen, small quantities of solid air	H/air > 17
21 – 50 K	Solid air, hydrogen gas	17 > H/air > 9
50 – 63 K	Solid air and liquid air (oxygen enrichment of liquid)	9 > H/air >6.75
63 5H/air liquid air	H/air ~6.75	
64 – 71 K	Liquid air, gaseous air (oxygen enrichment of liquid)	6.75 > H/air > 3.25
>71 K	Gaseous air	3.25 > H/air

The results in Table 1 apply to mixtures in which all of the phases remain in contact. The situation in the jet is more complex because of the potential for phase separation (especially the deposition of condensed liquids and solids).

Large volumes of liquid air will be formed in the outer parts of the hydrogen flow where the H/air ratio is in the range 6 to 14 and this material may drop out of the flow of gaseous hydrogen and residual gaseous air in which it was formed. Moving down it would typically come into contact with colder (more hydrogen rich), faster moving material. Droplets could be cooled back below the freezing point of air and even down to the boiling point of hydrogen, if they were deposited in an area where hydrogen was in sufficient excess. This would typically correspond to falling into the flow of liquid hydrogen close to the ground. This deposition process may substantially affect the transfer of heat and momentum to the lowest parts of the hydrogen gas and the liquid flow.

At least in principle this mechanism provides a means by which enrichment of oxygen in the liquid phase (which occurs for H/air ratios of around 8 and temperatures of around 66 K) may result in deposition of oxygen-enriched solid. Potentially these oxygen-enriched solids could be so cold that they could co-exist with liquid hydrogen.

It is of interest to calculate the maximum quantity of solidified air[2] with different compositions and temperatures that can be produced from the mass of liquid hydrogen released in Test 6 in RR987 (35.1 kg). Some results are shown in Table 2 (more details about the calculations are given in the appendix).

[2] Melting/freezing of mixtures of oxygen and nitrogen is discussed in the next section.

Table 2: Maximum quantities of solids (air and oxygen-rich air) that can be produced from 35.1 kg of liquid hydrogen under adiabatic, equilibrium conditions

Composition (mole % O2)	Final temperature (K)	Total solid (kg)	Oxygen (kg)
21	20 (boiling point of hydrogen)	29.6	6.9
21	58 (melting point)[3]	63.2	14.8
44[4]	20 (boiling point of hydrogen)	15.0	7.1
44	52 (melting point)	27.8	13.1

The figures in Table 2 can be compared with the estimates of solid production in Test 6 (17 +/- 5 kg) and oxygen consumption in the fireball 3.7 kg.

The production figures in Table 2 are upper limits, set only by energy conservation (in practice significantly less solid material could be produced). The two main potential reductions in efficiency are excessive dilution and heat transfer from the ground. These two factors are discussed below.

3.4.1 *Over-dilution*

If cold hydrogen gas (20.3 K) is mixed with air at a mole fraction of less than about 86% (H/air <6) then no condensation of air occurs and the hydrogen involved does not contribute to the production of solid in any way. Figure 14d shows that the density of mixtures is less than the overlying air (even if there is no rainout of liquid air) so there is no chance that stable density gradients will inhibit the mixing of the jet with air.

If the condensed air forms a fine aerosol that moves with the gas then the average velocity and hydrogen concentration are likely to follow the Gaussian distributions that are typical of momentum-driven mixing jets. This is shown in Figure 17 (it is assumed the hydrogen concentration is 100% immediately above the ground-level liquid flow and that the jet has radial symmetry). Also shown (red line) is the proportion of the flux of hydrogen that occurs beyond a specified radius. Comparing this fraction with the corresponding concentration shows what proportion of the hydrogen flux is associated with concentrations less than a given level.

[3] See Figure 23

[4] The figure of 44% has no fundamental significance. It is simply used to illustrate the effect on potential yields of oxygen enrichment. However, the figure is probably close to the level of enrichment above which ignition leads to detonation.

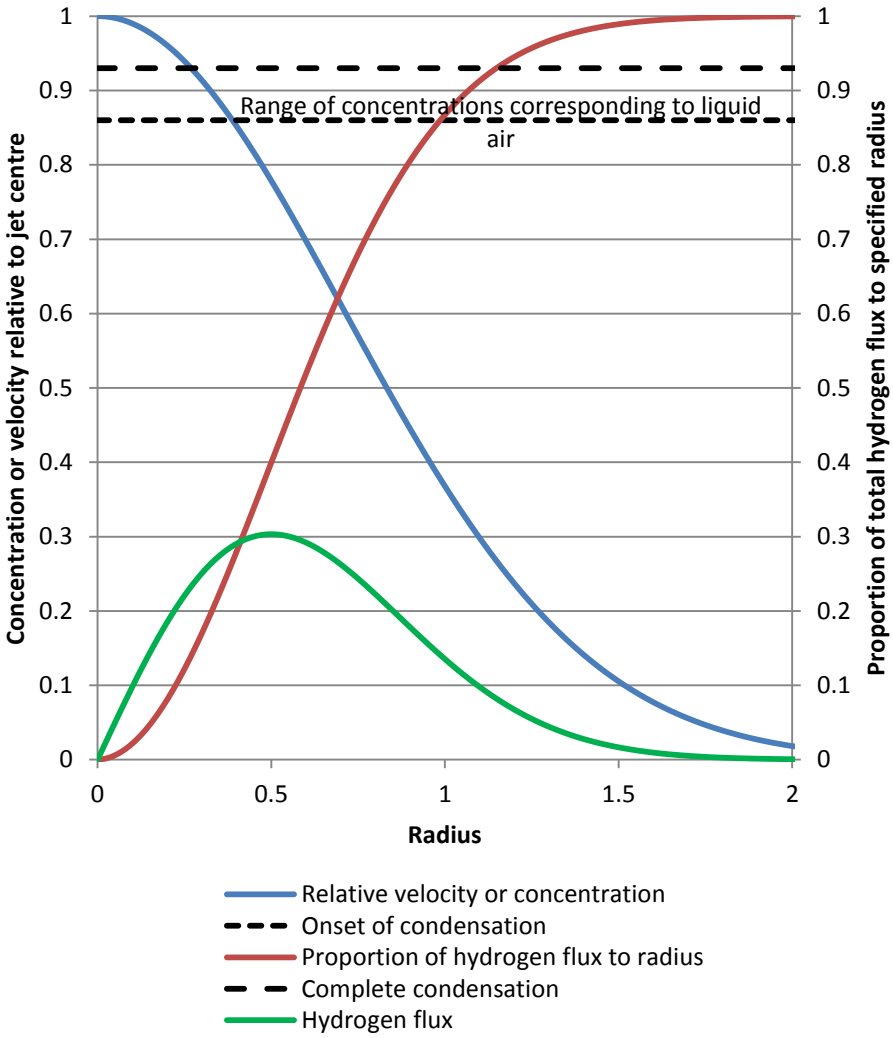

Figure 17: Hydrogen concentration, velocity and integrated flux (radial symmetry)

These results are illustrative only, the real flow will be strongly affected by the ground and a number of other complications. However, the analysis does show that a relatively small proportion of the hydrogen flux would be available to freeze air due to the narrow range of concentrations at which this occurs and the relatively low flux of hydrogen available across this range of concentrations.

Wind directions that are not aligned with the jet are likely to lead to more rapid mixing and consequently lower freezing efficiencies.

The relationship between entrainment of air, deposition and oxygen enrichment is discussed further in the final section of this report.

3.4.2 *Heat transfer from the ground*

Heat transfer from the concrete continues throughout the release, albeit at a reducing rate as the ground cools and the temperature gradient at the surface reduces. Figure 18a shows the results of typical results of 1-D numerical modelling of heat transfer within the concrete. It is assumed that the surface temperature, which is in direct contact with LH2, is at the boiling point of hydrogen. In this case, it assumed that the concrete below is at a

uniform temperature of 0°C at the start of the release. Figure 18b shows the heat transfer rate at the surface of the concrete over the period of the release.

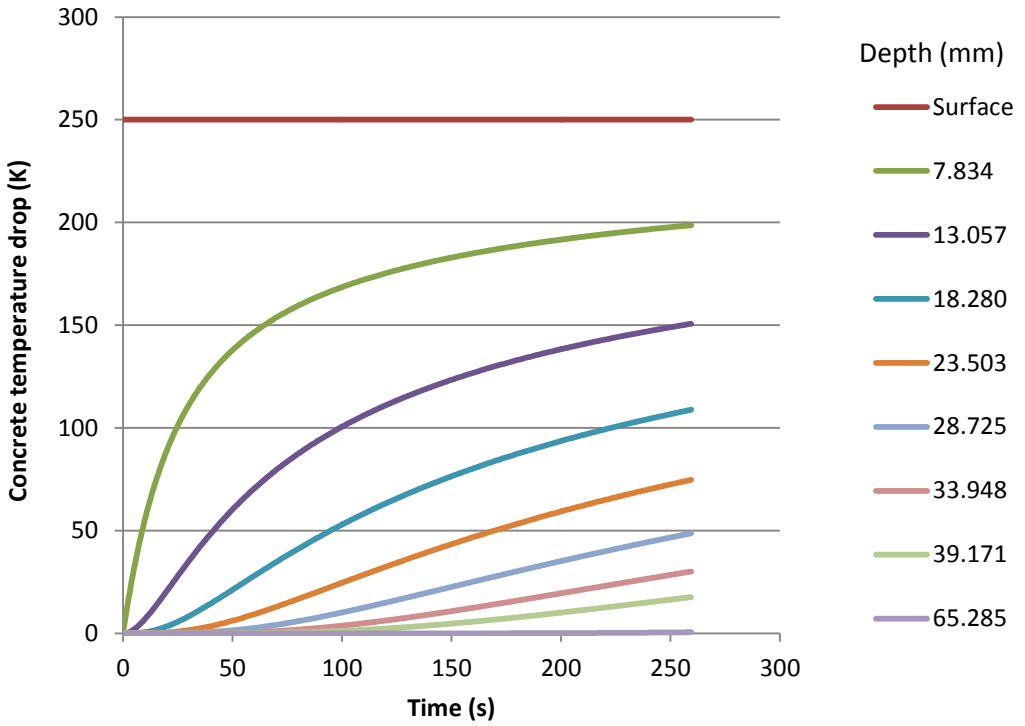

Figure 18a: Temperature drop distribution in the concrete as a function of time

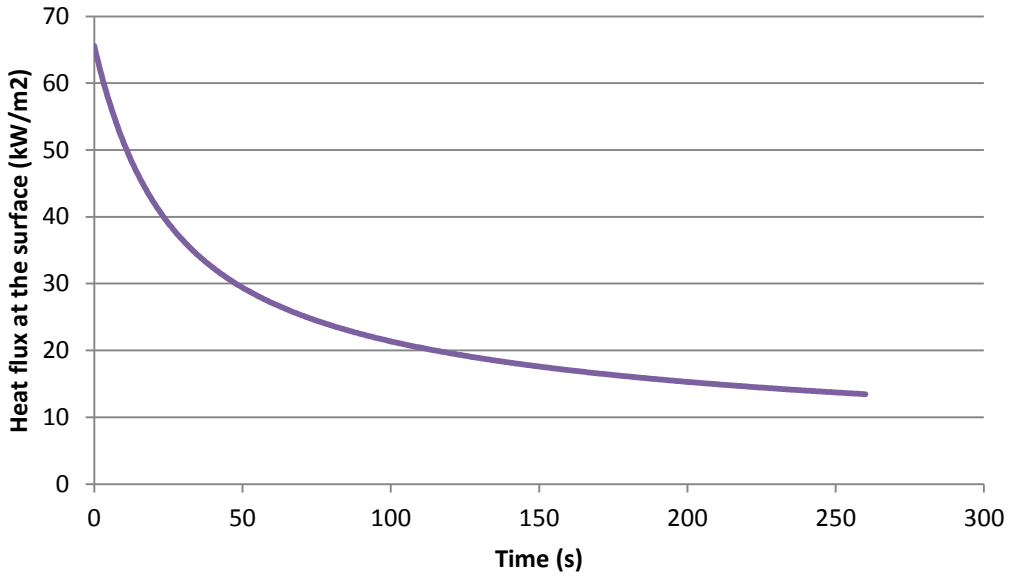

Figure 18b: Surface heat flux as a function of time

The area of contact between concrete and LH2 is around 1 m^2 (see Figure 12) so the final rate of heat transfer in Figure 18 corresponds to a LH2 vaporisation rate of around 13 x 2 / 0.9 = 29 g/s.

In fact, the concrete was pre-cooled to some extent by previous tests. Figure 19 shows how the total energy transferred from the ground varies with the initial concrete temperature. Also shown is the mass of hydrogen such a heat flux could vaporise and the proportion of the LH2 outflow in Test 6.

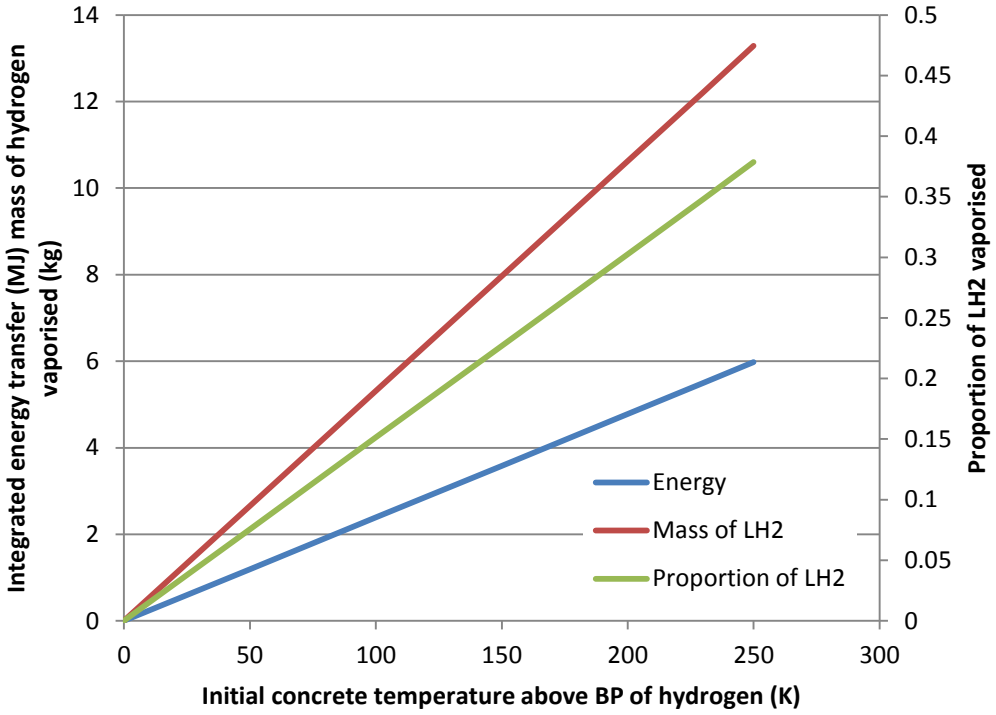

Figure 19: Integrated heat transfer to the ground and associated LH2 vaporisation

Given the delay between tests, it is likely that the ground temperature prior to Test 6 was only slightly below 0°C. This means that the overall loss of liquid hydrogen would have been around 35%.

Figure 20 shows how the energy transferred varies if the time of exposure is variable. In this case, the ground temperature has been assumed to be 0°C. This data was used earlier to estimate the yield of solid in Test 6 from a longer, unignited test – by comparing the energy transfers over periods of 260 and 420 seconds.

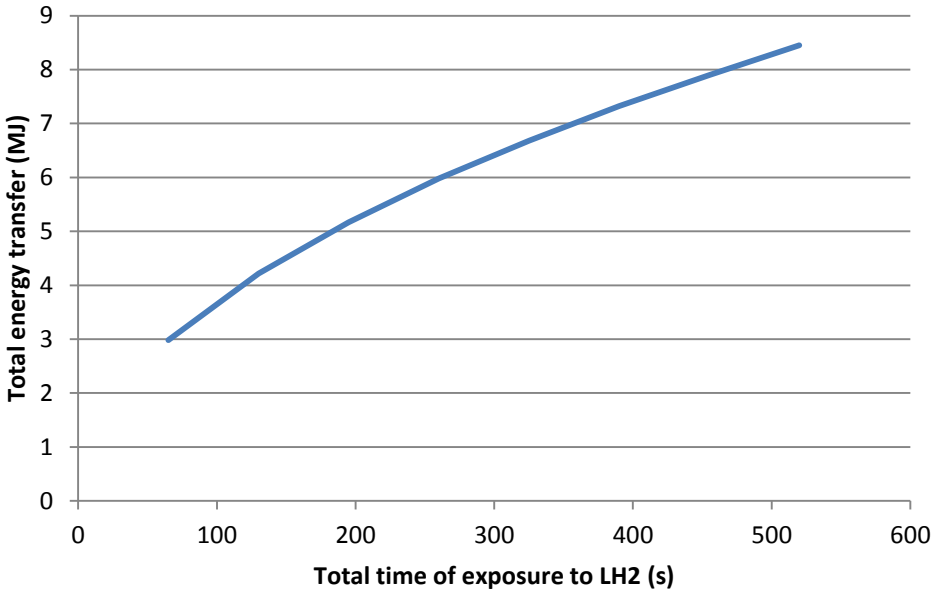

Figure 20: Energy transfer as a function of time of LH2 jet exposure

3.4.3 *Combined losses*

Overall, if it is assumed that the condensed air is fine enough not to settle out rapidly, it seems likely that the total yield of solid could only be a maximum of about 25% of the quantity calculated. This is based on ideal mixing in adiabatic conditions, with most of the liquid hydrogen not contributing to solid production because of over-dilution. For reference, the maximum yields of solids with different temperatures and compositions in Table 2 are reproduced in Table 3 with this efficiency factor applied.

*Table 3: Maximum quantities of solids (air and oxygen-rich air) that can be produced from 35.1 kg of liquid hydrogen, assuming an efficiency of **25%***

Composition (mole % O2)	**Final temperature (K)**	**Total solid (kg)**	**Oxygen (kg)**
21	20 (boiling point of hydrogen)	7.4	1.7
21	58 (melting point)	15.8	3.7
44	20 (boiling point of hydrogen)	3.75	1.8
44	52 (melting point)	6.9	3.3

The observed quantity of deposited solid (17 +/-5 kg) was apparently more than the total amount of solid that could be produced. If the efficiency of local deposition of a fine aerosol of condensation products were taken into account, the discrepancy would have been even larger.

This suggests that, in fact, the droplets and crystals produced were large enough to settle rapidly – on the time scale of transport along the jet. If condensed droplets of liquid air started to settle out as soon as they were formed, then they could have escaped the rapid over-dilution of the remaining gas phase. The losses associated with over-dilution would have been reduced and maximum production values may have substantially exceeded those in Table 3.

3.5 Conclusions about solid composition

A quantitative analysis of the effect of settling of droplets on the mixing processes in the jet and the efficiency of conversion of liquid hydrogen to solid air has not been attempted in this project but would be a useful next step in modelling.

Qualitatively, this kind of deposition process would have:

1. Increased the overall efficiency of solid formation;

2. Favoured the production of oxygen-rich condensed phases (as these formed first).

However, since the heat transfer from the ground accounts for around 35% of the LH2 vaporised, it seems unlikely that the overall efficiency could have been very much greater than 50%. Table 4 shows the maximum yields in this case.

*Table 4: Maximum quantities of solids (air and oxygen-rich air) that can be produced from 35.1 kg of liquid hydrogen, assuming an efficiency of **50%***

Composition (mole % O2)	**Final temperature (K)**	**Total solid (kg)**	**Oxygen (kg)**
21	20 (boiling point of hydrogen)	14.8	3.5
21	58 (melting point)	31.6	7.4
44	20 (boiling point of hydrogen)	7.5	3.6
44	52 (melting point)	13.8	6.6

The low yields of solid in the oxygen-rich cases (data rows 3 and 4 in Table 4) arise because only about 30% of the air condenses at a mole fraction of 44% O2 (see Figure 13a and 13b). Excess cold, nitrogen-rich gas is also produced which requires the vaporisation of large amounts of liquid hydrogen but does not contribute to the accumulated solid.

The potential yields of solids above the boiling point of hydrogen (data rows 2 and 4 in Table 4) are higher than for the colder material because a given quantity of liquid hydrogen is capable of absorbing more heat from air (it must first be vaporised and then heated to the final temperature).

Oxygen enriched solid cold enough to mix with liquid hydrogen

Comparing the figures in the third data row of Table 4 with the observed mass of deposit (17 +/-5 kg), it seems that if the observed solid was oxygen-enriched then only a small proportion could have been at the boiling point of hydrogen.

There might be a small amount of cold material of this sort (at 20.3 K) at the front of the mass, but most of such an oxygen-rich solid must be warmer and this means it could not be in contact with liquid hydrogen and therefore could not contribute to a condensed phase detonation. The small quantity of material that could be cold enough to be mixed with liquid hydrogen could not, in itself, contain sufficient oxygen (3.7 kg) to account for heat release in the fireball.

The temperature of deposits and their LH2 content depends on the release geometry. If solids accumulate where LH2 is in large excess (e.g. a confined jet) then the mass of solid air would incorporate LH2. Ignition tests by HSL (see RR987) on samples of the solid

collected showed that they could support a flame but did not exhibit rapid or explosive burning.

Solid air cold enough to mix with liquid hydrogen

Comparing the figures in the first data row of Table 4 with the observed mass of deposit (17 +/-5 kg), it seems that it is possible that all of the solid could be in contact with liquid hydrogen if it had the composition of air. If detonated it could have sufficient oxygen to account for the observed fireball. There is no reason why oxygen enrichment would be expected in any part of such a mass.

Warmer oxygen enriched solid

It is possible that the bulk of the solid was oxygen-rich to a level of 44% mol/mol but at a significantly higher temperature – close to the melting point (see fourth data row of table 4). This solid would also contain more than the amount of oxygen that contributed to the explosion.

Warmer solid air

The potential yield of solid air (not oxygen-enriched) is much greater than was observed and would contain sufficient oxygen to sustain the observed explosion.

In all cases, the solids would also have probably contained a small proportion of condensed water. This might have significantly affected their potential to absorb thermal radiation after ignition.

3.6 Mechanics of solid production

The jet of LH2 would have vaporised as it moved away from the nozzle because of thermal contact with the ground and entrained air. The resulting flow of cold gaseous hydrogen mixed with air and caused substantial condensation. The analysis presented here indicates that a high proportion of the initially entrained air was locally deposited – suggesting the growth of larger droplets that fell out rapidly rather than being carried away and further diluted with air.

Figure 21 shows schematically how the growth of a solid deposit might have proceeded.

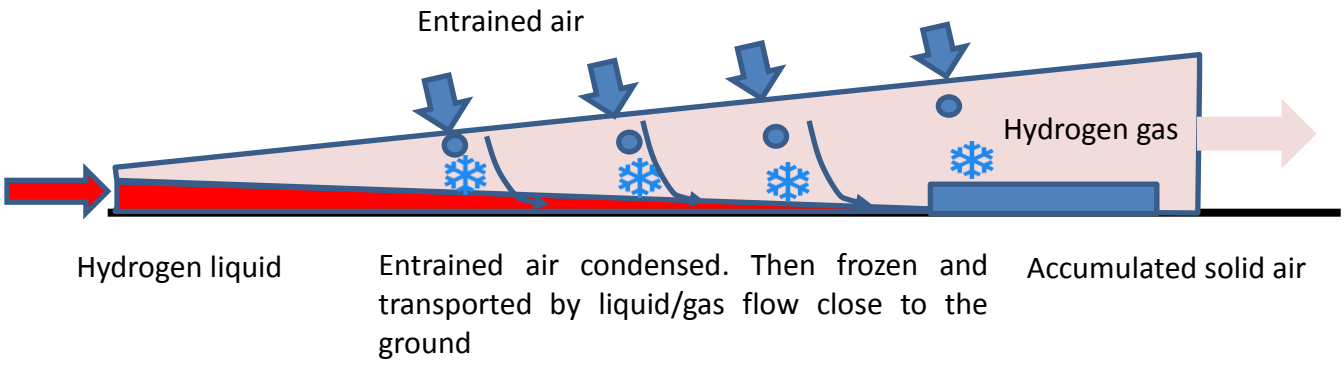

Figure 21: Schematic showing how solid deposits may accumulate

As the heat transfer from the ground slackened, the primary source of heat to the LH2 flow at ground level must have been entrained condensed air. If this were in the form of deposited droplets, then this would explain why the efficiency of capture and freezing

was so high: the liquid would have persisted, spreading along the ground, until a sufficiently high proportion of condensed air had been deposited to complete the vaporisation process.

The final resting place of deposited frozen droplets falling into the liquid would be at the limit of the rapid liquid flow and this does seems to correspond to the distribution of solid shown in Figure 10.

The accumulation of solids itself would eventually impede the flow of liquid along the ground and it may be that backing up of LH2 led to a widening of the area where solid was distributed and a gradual shift in the front edge of the deposit closer to the source.

Not all of the droplets of condensed air would fall on the liquid; some would fall out beyond this point, especially as extent of the liquid flow was restricted. In this case deposits (potentially well above the BP of hydrogen) would fall out on colder previously deposited material. This would produce a larger amount of solid deposit at a temperature above the BP of hydrogen. Overall, only a proportion of the deposited material would have been cooled to LH2 temperatures. The remainder would have been cooled to the final higher temperature by exchange of heat after falling out.

The energy balance arguments presented previously support this conclusion. If all of the solid deposited was at some point cooled to liquid hydrogen temperatures then tight limits on production masses apply and the observed high yields of solid remain to be explained.

The height profile of the mass of solid at the end of the flow is also consistent with this picture. Moving back from the front, the depth of solid appears to increase – which would correspond to the continued deposition beyond the limit of liquid flow.

It seems that towards the end of the test the majority of the solid mass would have been significantly above the boiling point of hydrogen. However, solids right at the front of the mass would have still been in contact with liquid hydrogen.

3.7 Physical form of the solid accumulation

If it is correct that the bulk of the solid is not in contact with fresh liquid hydrogen then continuing heat transfer from the ground to the base of the solid deposit would have tended to cause progressive erosion by melting and vaporisation – partially offsetting the accumulation by deposition on the upper surface. It is possible that such erosion did not occur uniformly but allowed the development of a network of cavities in the solid immediately above the ground.

Prior to ignition, these cavities might have contained gaseous hydrogen, air or a mixture. They might also have allowed the percolation of liquid hydrogen under the solid if the reach of the liquid flow increased after ignition.

In the absence of contact with LH2, ongoing heat transfer from the ground would have led to significant vapour production and it is possible that escape of this warmer gas could have resulted in the formation of an array of vents leading from cavities immediately above the ground to the surface of the solids.

4 Part 3: Post-ignition behaviour of solid phase materials

After ignition, there was a sustained jet fire for all of the time (~3.5 seconds) before the secondary explosion. This jet fire must have consumed much of the additional hydrogen released over this period. The hydrogen involved in the secondary explosion (460 g = 6.5 litres liquid) must therefore have included some material that had accumulated previously – in a form and a location that could become involved in the secondary explosion. There are several quite distinct explanations for this, involving quite different kinds of explosion.

1. **Condensed phase detonation reaction:** The hydrogen may have accumulated as a liquid that was intimately mixed with accumulated solid oxygen-enriched air. This mixture may be capable of detonating if sufficiently strongly shocked or, more likely; in this case, it may exhibit DDT following thermal initiation. The first explanation is therefore that the secondary explosion was a condensed phase detonation reaction.

2. **Gas-phase deflagration in the open:** The hydrogen may have accumulated in the ground flow between the nozzle and the solid. This material would have been exposed to thermal radiation after ignition and any vapour released may not have been immediately ignited (since it was not in contact with air). Further from the nozzle, oxygen-enriched air may have been released *beneath* this flow of hydrogen gas. It is possible that the secondary explosion occurred when there was delayed ignition of these gases downstream. The second explanation is therefore that the secondary explosion was a fast gas-phase deflagration in the open.

3. **Confined deflagration**: It is possible that the solid deposit was porous – especially where it contacted the ground – and that, after ignition, low-level cavities became flooded with liquid hydrogen. Melting of oxygen-rich solid deposits after ignition could also have introduced highly oxygen-rich liquid into these spaces via drainage through cracks. It is possible that a fast deflagration propagating in mixed LH2 and air could have generated overpressures high enough to disperse the overlying solid air into the gaseous hydrogen flow above. Flammable mixtures formed in this way could have been highly turbulent and supported very rapid combustion, although they would not have been fully pre-mixed.

4. **Rapid phase transition**: There may have been a rapid phase transition involving contact between superheated LH2 and liquid air. Such an event would have been potentially immediately followed by a rapid combustion reaction.

A necessary prequel to considering the relative merits of these potential explanations is an analysis of the fate of hydrogen and oxygen in gaseous, liquid and solid phases during the period following ignition.

4.1 Post-ignition behaviour of hydrogen

Heat flux measurements made as part of the work described in RR987 suggest that the average heat flux from the jet fire and flash fireball to the area of ground in front of the jet covered by liquid hydrogen or solid air was approximately 50 kW/m^2.

The area of ground covered by liquid hydrogen between the nozzle and solid deposit was approximately 1 m^2 and the time of exposure between ignition and the secondary explosion was 3.5 seconds. The total radiant input to the surface of the pool was consequently approximately 175 kJ. Given the heat of vaporisation of hydrogen is 450 kJ/kg radiant heat could *in principle* have vaporised an additional 400 g of hydrogen (with low momentum).

In addition, the hydrogen jet would have supplied a further 475 g during the period of burning prior to explosion. It is reasonable to expect that some of this hydrogen might not have burned at the time of the secondary explosion – since much of it would be a ground level liquid flow or very rich gas flow that would not have mixed with overlying air.

However, it is not clear how much of the thermal radiation would actually have been absorbed by a relatively thin layer of liquid hydrogen. Hydrogen is very transparent in the infrared[5] – much more so than other fuels. If most of the thermal radiation was transmitted and had to heat the concrete first before increasing the rate of vaporisation indirectly, the positive effect on vaporisation over a few seconds would have been be small.

It is not clear how flames at the top of the hydrogen flow would have affected the convective component of pool vaporisation. Mixtures close to the surface would have been dense and well above the UFL of hydrogen: direct contact between the flame and the LH2 surface may not have occurred. It seems likely that a ground level flow of LH2 would have continued to impinge on part of the accumulated solid.

4.2 Post-ignition behaviour of oxygen

Solidified air clearly accumulated in large quantities and the previous sections showed that this might have been significantly oxygen enriched. The analysis also suggested that if there was a moderate level of oxygen enrichment then only a small proportion could have been cold enough to coexist with LH2.

In addition, there is a possibility that the jet fire preceding the explosion would have affected the solid – potentially melting a proportion of the material and thereby changing the composition and location of oxidants encountering LH2 or vaporising.

4.2.1 *Rate of solid surface regression*

Two methods have been tried to estimate the potential rate of surface regression of the solid:

[5] M. G. Zabetakis and D.S. Burgess *Research on the hazards associated with the production and handling of liquid hydrogen, US* Bureau of Mines Report 5707.

Energy balance:

Heat input to all solid surfaces over the period of the jet fire ~ 100 kJ

(50 kW/m^2 for 3.5 s over an exposed area[6] of 0.6 m^2)

Heat of fusion of oxygen 13.7 kJ/kg

Potential total melt 7.3 kg (if solid close to the melting point)

Regression rate (assuming a density of 0.9 kg/m^3) = 4 mm/s

PRESLHY observations:

Solid deposits built up on instrumentation supports close to the nozzle in some PRESLHY trials. These were observed to regress by very rapid melting at a rate of approximately 1 mm/s (Figure 22).

Figure 22: Solid deposits melting rapidly after PRESLHY trials

Forced heat transfer coefficients are not easy to determine in this case but a figure of around 30 W/K/m^2 seems plausible which would correspond to a heat transfer rate of about 6.5 kW/m^2.

Heat transfer and regression rate are probably much higher when the condensed air deposits (including a proportion of ice crystals) are affected at quite close range by a jet fire. If the heat transfer rate from the flames is of the order 50 kW/m^2 then it seems reasonable that the regression rate might be 4 mm/s so that 7 kg of oxygen–rich solid could be *melted* by the jet fire in 3.5 seconds.

This is a substantial rate of melting and there would be rapid draining of the liquid from the surface of the accumulated solid. Some would flow off the edge of the solid towards the jet, possibly coming contact with LH2.

[6] Including areas at the end and sides of the jet

Liquid air would also flow out around other parts of the periphery of the accumulated solid and spread out rapidly across the concrete. High rates of heat transfer could be expected for contact between oxygen enriched liquid air and areas of concrete not previously exposed to the jet. It seems reasonable to expect that there could be rapid vaporisation of liquid for a few seconds. The source of heat for this process would be (primarily) heat stored very close to the surface of the concrete.

It is also possible that some liquid penetrated vents in the accumulated solid (caused by escaping gas) and potentially drained into cavities immediately above the ground

4.2.2 *Composition of the melt*

A liquid/solid phase diagram for nitrogen/oxygen is shown in Figure 23.

The first liquid produced as the solid melts is significantly enriched in oxygen. If the initial molar concentration of oxygen in the solid is between about 53% to 77%, the liquid formed has the eutectic composition (77% oxygen). For lower initial oxygen mole fractions, there is also significant enrichment. Figure 24 shows that for a solid oxygen concentration of 44%, the first liquid would have a concentration of around 70% oxygen.

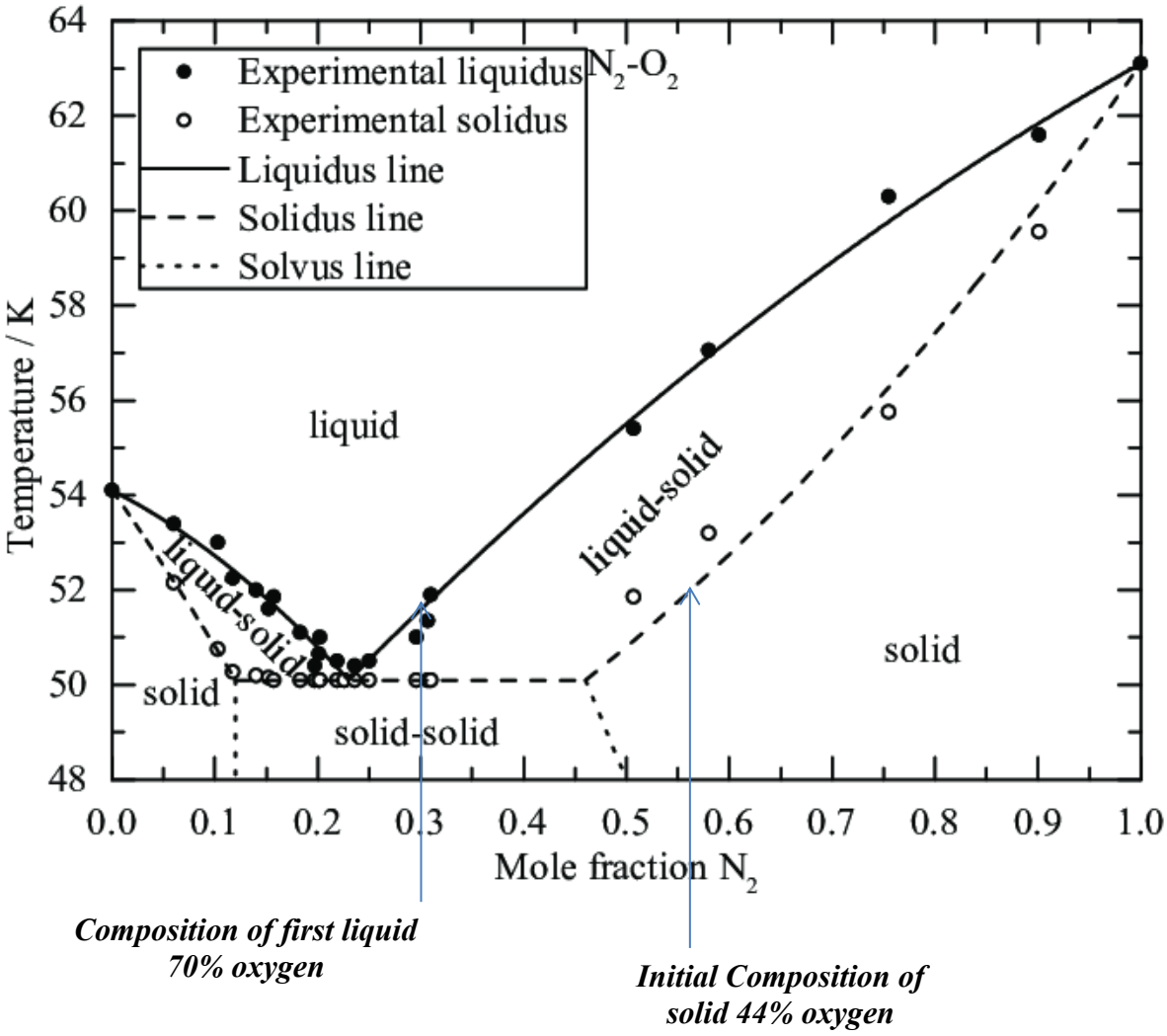

Figure 23: Phase diagram for mixtures nitrogen and oxygen

Overall, it seems reasonable to assume that a substantial amount of oxygen-enriched *liquid* air (up to about 70% oxygen) would have been produced and could have encountered LH2. It is also possible that a significant part could have been vaporised at ground level by contact with relative warm concrete.

4.3 Condensed phase detonation reaction

4.3.1 *Triggered by external pressure*

Solid air (normal composition) mixed with excess liquid hydrogen can be detonated with an explosive booster providing an initiating pressure of 7-10 kbar[7].

Attempts by the Bureau of Mines to initiate this mixture mechanically with high-speed projectiles was not successful but oxygen-enriched mixtures were more sensitive (Table 5).

Table 5: Initiation of solid oxygen /nitrogen mixtures in excess liquid hydrogen

Percent N_2 in solid (mol/mol)	**Initiation velocity (ft/s)**
0	1660
23	2280
47	3580
78	Insufficient velocity available

It would appear that if the solid component has the composition of air (no oxygen-enrichment); the mixture with LH2 is very resistant to mechanical initiation.

There are few if any obvious candidates for extremely energetic initiators in the post-ignition phase of the liquid hydrogen jet.

Thermal stresses in the solid air could cause cracking but this is unlikely to generate significant energy if the material were porous and capable of forming intimate mixtures with liquid hydrogen. There was no evidence of spalling of concrete.

One possible exception might be a rapid phase transition resulting from contact between LH2 and liquid air. This is discussed separately and might explain the observed explosion even if it were not capable of triggering a solid phase detonation.

Overall, the probability that the explosion was a detonation triggered by shock appears extremely remote.

[7] Fire and Explosion Hazards of Flight Vehicle Combustibles, Litchfield, E. L. and Perlee, H.E. Bureau of Mine Progress Report April to June 1964.

4.3.2 *Spontaneous deflagration to detonation transition*

Previous experience with the combustion of mixtures LH2 and oxygen diluted with varying amounts of nitrogen have shown that DDT is a possible outcome of ignition, especially for moderate to high levels of oxygen enrichment.

A section of the review by Litchfield and Perlee[8] is reproduced below:

> **Spontaneous Transition from Deflagration to Detonation:**
>
> Samples containing 0.7 and 1.0 oz of oxygen and an excess of liquid hydrogen were ignited to deflagration by firing an electric match in the hydrogen-air vapor space. Transition to detonation occurred after some appreciable delay time but in the absence of any confinement beyond that supplied by the mixture container. The delay times were of the order of one minute and are believed to correspond to the times required for the fire to consume the liquid hydrogen and expose the liquid hydrogen-crystalline oxygen interface. In the absence of diluents, detonation always resulted and the blast, as indicated by strip gage deflection, was equivalent to that obtained with projectile initiation of detonation. Transition must thus have occurred before any significant consumption of the explosive mixture in deflagration.
>
> Samples containing 0.7 oz oxygen and diluted with nitrogen or methyl chloride detonated, after initiation to deflagration, up to dilutions of 45 and 50 weight percent of total solids, respectively. At dilutions of 50 and 65 weight percent, respectively, the samples burned to completion without detonation. Failure to achieve detonation at these larger dilutions must be attributed to the existence of a subcritical sample size. Larger samples have given transition to detonation with nitrogen dilutions of 50 weight percent.

This experience suggests that spontaneous transition to detonation is a possible outcome where air enriched to more than about 50% oxygen is in contact with LH2. This happens in effectively unconfined conditions.

It seems quite credible that solid air with the necessary level of oxygen enrichment could have encountered LH2 in the RR987 test either:

i) Through direct deposition from the gas phase prior to ignition. The yield of material with such a high level of oxygen enrichment would have been fairly low.

ii) During a melt-flow process after ignition. Levels of oxygen enrichment could have been significantly higher than in the material originally deposited but again the quantity would have been quite small.

It is possible that DDT involved relatively small amounts of mixture with the right composition but that the detonation once initiated was able to spread to larger quantities with somewhat lower levels of oxygen enrichment.

The effect of a detonation would have been to violently disrupt any non-detonable solid air; dispersing it rapidly in the overlying flow of hydrogen. The result could have been an extremely rapid secondary gas phase explosion that may have contributed to the overall size of the fireball.

---

[8] Litchfield and Perlee, (1965) *Fire and Explosion Hazards of Flight Vehicle Combustibles*, Tech Rep AFAPL-TR-65-28

4.4 Fast gas-phase deflagration

Hydrogen cannot entrain oxygen from overlying ambient air without the fuel being immediately consumed by the jet fire. However, during the jet fire there is another possible source of oxygen in the accumulated, solidified air. If this is vaporised it might form a bubble of premixed flammable gas that was isolated from the flame by a blanket of hydrogen that was over the UFL.

The previous analysis showed that a substantial amount of oxygen-enriched *liquid* air could have been produced and that a significant part of that could have been vaporised at ground level.

The gas would have been relatively dense and initially at rest relative to the ground, however, there might have been some mixing with the gaseous hydrogen flow above. The development of a mixed unignited flow of flammable, oxygen-enriched gas under the hydrogen flow is illustrated schematically in Figure 24.

The hydrogen rich layer would be progressively eroded by entrainment of additional air and eventually, the surface corresponding to concentrations at the UFL, would come down to ground level. However, within this envelope a flammable bubble could develop at low level.

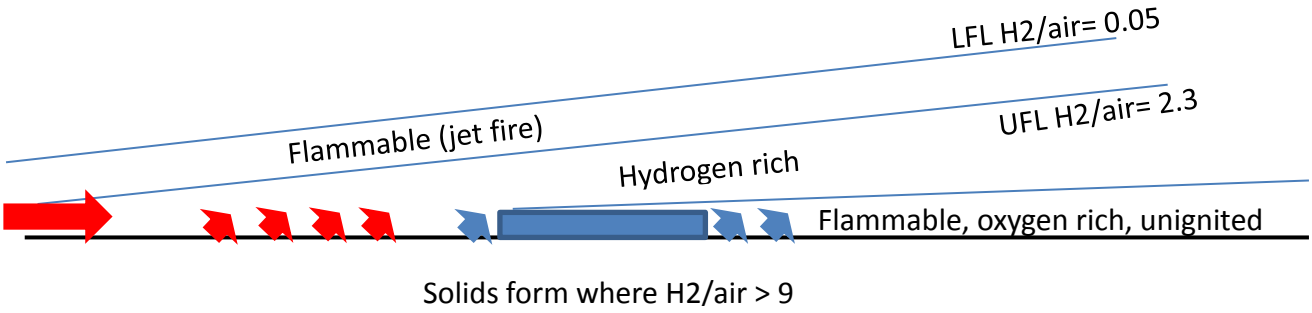

Figure 24: Schematic showing development of a flammable mixture under the hydrogen flow. Red arrows indicate hydrogen input, blue arrows indicate oxygen enriched air

The volume of oxygen-enriched air at around 90K required to fully account for all of the oxygen in the observed explosion is of the order 1 m^3. A bubble of flammable gas about a metre wide would therefore have had to extend several metres downstream and have a depth of a few tens of centimetres.

There are some significant problems with this deflagration explanation for the secondary explosion.

1. It is not clear that thermal radiation could have driven the necessary vaporisation rates - especially for hydrogen – see the discussion in Section 4.1.

2. The stability of the dense flow of vaporised air would have inhibited mixing with the overlying, rather sluggish, hydrogen flow. Initial turbulence levels and flame speeds would have also been reduced.

3. The total amount of excess gaseous hydrogen available to separate the flammable region at the top from a flammable pocket below would have been limited. It is difficult to see how there could have been enough to effectively surround a pocket containing 1 m^3 of air. The depth of the flow would have had to be very small compared with its width.

Possibly, smaller amounts of vaporised air could have been involved in the original premixed explosion in a smaller pocket - with the remainder being rapidly entrained by the fireball.

Overall this analysis suggests that vaporisation of significant amounts of oxygen-enriched air is possible during the jet fire and this might occur in some areas where the overlying gas was above the UFL leading to some accumulation of flammable mixtures. However, the mechanism does not look to be a likely candidate for the explosion observed in RR987.

4.5 Deflagration reactions under the solid deposit

It is possible that there were cavities within the solid – especially where it contacted the ground – and that these cavities could have become flooded with liquid hydrogen after ignition. Melting of oxygen-rich solid deposits after ignition could also have introduced highly oxygen-rich liquid into these spaces via drainage through cracks.

It is possible that a fast deflagration propagating in areas where LH2 and solid air were mixed could have generated overpressures high enough to disperse the overlying solid air into the hydrogen gas flow above. Flammable mixtures formed in this way could have been highly turbulent and supported very rapid combustion, although they would not have been fully pre-mixed.

4.5.1 *Deflagration fundamentals*

The laminar burning velocity in a premixed gas[9] is of order:

$V_{lam} = \sqrt{\frac{k}{\rho C_p \tau_b}}$ k is the thermal conductivity, τ_b is the reaction time for burning

For hydrogen/air, τ_b is around[10] 3 x10^{-6} s and the laminar speed predicted of order 2 m/s.

Turbulence accelerates the flame by increasing the area of contact between burned and unburned gas i.e. the flame area. The turbulent burning velocity in the open can be of order 5-10 m/s.

The flame speed depends on the relative confinement of burned and unburned gas. If the burned gas is confined (e.g. propagation away from the open end of a tube towards a closed end) the flame speed is close to the burning velocity. If the unburned gas is confined (e.g. propagation away from the closed end of sealed tube) the burning velocity is magnified by expansion of the burned gas. Flame speed will exceed the burning velocity by the expansion ratio.

[9] Bray, K.N.C. *Turbulent flow with pre-mixed reactants* In Turbulent Reacting flows Eds Libby, P.A. and Williams F.A., 1980, Springer.

[10] Osipov et al NASA 1012.5135 https://www.osti.gov/pages/servlets/purl/1371474

Obstacles increase the flame speed by increasing the turbulence levels in unburned gas driven forwards ahead of the flame. The flame may also divide as it passes an obstacle, further increasing the flame area.

4.5.2 *Condensed phase deflagration in LH2/air mixtures*

The propagation of deflagration into a mixture of LH2 and solid air is much more complicated. Reaction would be in the gas phase but there would be rapid generation of bubbles close to the reaction zone and other multi-phase phenomena. However, similar arguments about the progress of the thermal front into the liquid suggest that the rate of the reaction should still be fairly slow.

No reports of systematic measurements of burning velocity for deflagration of LH2/air mixtures have been found but the text reproduced previously from the review by Litchfield and Perlee seems to imply that non-detonative deflagration reactions are relatively slow "burning" events. Mixtures with higher oxygen content are prone to DDT, as noted previously.

Overall it seems very unlikely that a stable deflagration, fast enough to generate the observed pressure effects, could propagate though a significant amount of material without giving rise to DDT.

4.6 Rapid phase transition (RPT)

The effect of thermal radiation on a liquid hydrogen flow may be to produce a general warming through the whole depth. Vaporisation at the lower boundary may be slow because of an insulating vapour film. In principle, the temperature through the whole depth could be raised well above the normal boiling point of hydrogen making the fluid more susceptible to being involved in a RPT event.

The jet fire in Test 6 would have prevented (unburned) air coming into contact with the top surface of the hydrogen gas flow and would consequently have stopped the deposition of condensed air into the liquid that might otherwise have served to nucleate boiling.

At the same time, the effect of thermal radiation on the exposed solid would have been to produce oxygen- enriched *liquid* air on the top surface. Some of this would have flowed off the edge of the solid and along the ground underneath the accumulating LH2 – the slope of the top surface of the solid could promote this. Solid air deposits both at the end and the sides of the hydrogen pool may have contributed to this undercutting flow of liquid air.

It is conceivable that an RPT could have occurred, without any significant mechanical trigger, in these circumstances. The rapid vaporisation and associated shock would be likely to have led to mixing of hydrogen with overlying air and potentially accumulated oxygen-enriched liquid and solid air. Such a mixture would be susceptible to violent secondary combustion.

5 Tests at KIT

As part of the PRESLHY project Karlsruhe Institute of Technology (KIT) have carried out some LH2 pool evaporation and burning trials. Full details of this work were not available at the time of writing but some qualitative observations have been shared and are significant in the context of the study of condensed phase explosion risks.

LH2 was released onto at least three types of surface – contained in lightweight, insulated steel trays (500 x 500 mm):

1. Concrete;
2. Sand;
3. A 150 mm deep bed of rounded stones (Rheinkies – Size ~ 50 mm).

A layer of LH2 (of order 100 mm deep) was established in the trays above the various surfaces and the subsequent rate of vaporisation or burning was measured.

In the case of the concrete and sand surfaces, the LH2 layer burned away steadily without any explosive effects.

In the case of the bed of stones, a violent explosive event occurred within a few tens of milliseconds of ignition. The stones were ejected with velocities of several hundreds of metres per second and the steel tray was bowed out and torn apart along some weld lines.

The violence of the explosion suggests that a condensed phase reaction occurred within the bed of stones.

It is interesting that the explosion occurred almost immediately after ignition. This is in contrast to the tests described by Litchfield and Perlee where overlying LH2 burned off before the flames contacted crystalline air saturated with LH2, triggering a condensed phase reaction and rapid DDT. There seem to be two possibilities to explain the immediate explosion in the KIT test – both of which depend on a fairly vigorous level of residual vaporisation at depth, driven by heat transfer from the stones or tray. In this case it is possible that

1. A strong bubble flow through channels in the stones or close to the tray wall could mix air crystals into the overlying LH2, where the mixture contacted the flame.

Or

2. A gas explosion could propagate down through a continuous stream of venting hydrogen/air close to the tray wall. The flame would propagate down into the overlying LH2.

Another interesting observation is that although the tray was torn apart, it was not reduced to shrapnel – which is a common consequence of a condensed phase detonation. However, it might be premature to dismiss the possibility of detonation solely on this basis. It is possible that detonable mixtures did not extended right down to the bottom of the tray and were separated from the tray wall by a layer of vapour. In this case the strong pressure gradients associated with a detonation would have been somewhat moderated.

In fact the contact zone between a bed of rounded stones and the wall provides a low resistance venting path and in a fairly small tray it might be expected that a high

proportion of the vented gas from the lower parts of the bed would escape this way. A vapour layer with a thickness comparable to the stone size could be expected.

In the KIT test, there was clearly no time for significant radiative melting of solids and in any case, any condensed air was submerged in LH2. It must be the case that the condensed air deposited in the tray was already sufficiently enriched in oxygen to react violently.

Details of the filling process during which air deposition occurred are not known (e.g. location of release point, liquid outflow speed and orientation, wind conditions etc.). However, the flow conditions and impacted surface were obviously completely different to those in the HSE RR987.

It seems that ground level jet releases of LH2 in a fairly wide range of circumstances may allow the accumulation of condensed air with a composition that has the potential for violent explosion. This may have to be another ingredient of risk assessment for such events alongside jet fire and vapour cloud explosions.

More experimental and modelling work to investigate the mixing and deposition of solid air during contact with cryogenic hydrogen is required. It would be particularly important to know how the risk changes with the scale of release.

6 Conclusions

6.1 Deposition of solids from a low pressure ground level jet of LH2

1. After an initial period, the main source of heat input to liquid on the ground comes from entrained air.

2. This heat input is in the form of direct contact with air/GH2 and deposition of droplets and crystals of condensed air into the liquid.

3. Deposited crystals of solid air are transported by the liquid flow – coming to rest where the liquid flow is sufficiently shallow and slow.

4. Some deposition of air occurs beyond the edge of the liquid LH2 flow and this adds to the mass of solid air formed, whilst raising its temperature above the boiling point of hydrogen.

5. Moderate levels of oxygen enrichment can occur during the condensation of air.

6. The temperature and chemical composition of solids formed from releases of LH2 are likely to vary significantly with wind conditions and release geometry. Low relative speeds between GH2 and air could allow buoyancy stabilisation of a condensation zone where the temperature was fairly close to the initial boiling point of air and the condensed material was oxygen rich.

7. In the HSL 2010 tests in which a secondary explosion was observed, the large quantity of solid observed means only a small proportion could have been both significantly oxygen-enriched and cold enough to form an intimate mixture with liquid hydrogen.

6.2 Post-ignition

1. LH2 only absorbs thermal radiation weakly and it is likely that the jet fire did not prevent contact between a ground level flow of LH2 and accumulated solid air.

2. Thermal radiation has the potential to melt large quantities of solid air rapidly – regression rates could be several mm per second. Further oxygen enrichment of the melt to a level of around 70% mol/mol is possible.

3. Mixtures of LH2 with solidified air enriched to over 50% oxygen mole/mole are prone to rapid DDT if ignited. This is the most likely explanation for the observed secondary explosion in RR987.

4. An explosion also occurred in PRESLHY tests at KIT that was almost certainly a condensed phase reaction between solid air and LH2. The surface material and discharge conditions were completely different to those in the RR987 tests. It seems that ground level jet releases of LH2 in a wide range of circumstances may allow the accumulation of condensed air with a composition that has the potential for violent explosion. This may

have to be another ingredient of risk assessment for such events, alongside jet fires and vapour cloud explosions.

5. More experimental and modelling work to investigate the mixing and deposition of solid air during contact with cryogenic hydrogen is required. It would be particularly important to know how the risk changes with the scale of release.

7 Appendix 1: Mass flow rates in the PRESLHY and RR987 tests

7.1 Summary

Table A1 shows flow rates measured in PRESLHY tests

Pressure	Nozzle size	Mass flow
5 bar	6mm (¼ ”)	90-100 g/s
5 bar	12mm (½”)	265 g/s
5 bar	1” (open pipe)	298 g/s
1 bar	12mm (½”)	104-107 g/s
1 bar	1” (open pipe)	135-144 g/s

Some values (for smaller nozzles at high pressure) are known with confidence from a mass flow meter.

In other cases (low pressure and/or open pipe) the mass flow meter saw a 2-phase flow with a high void fraction and did not give reliable output. The mass flows can, however, be deduced (within a range) from pressure measurements.

The mass flow in previous work on solid accumulation used much of the same equipment and the PRESLHY data can be used to estimate the flow rate in these experiments at approximately 135 g/s.

This figure is of significance in interpreting the observations of the rate solid deposition.

For reference, a close up of the PRESLHY set-up including the measurement section is shown in Figure A1.

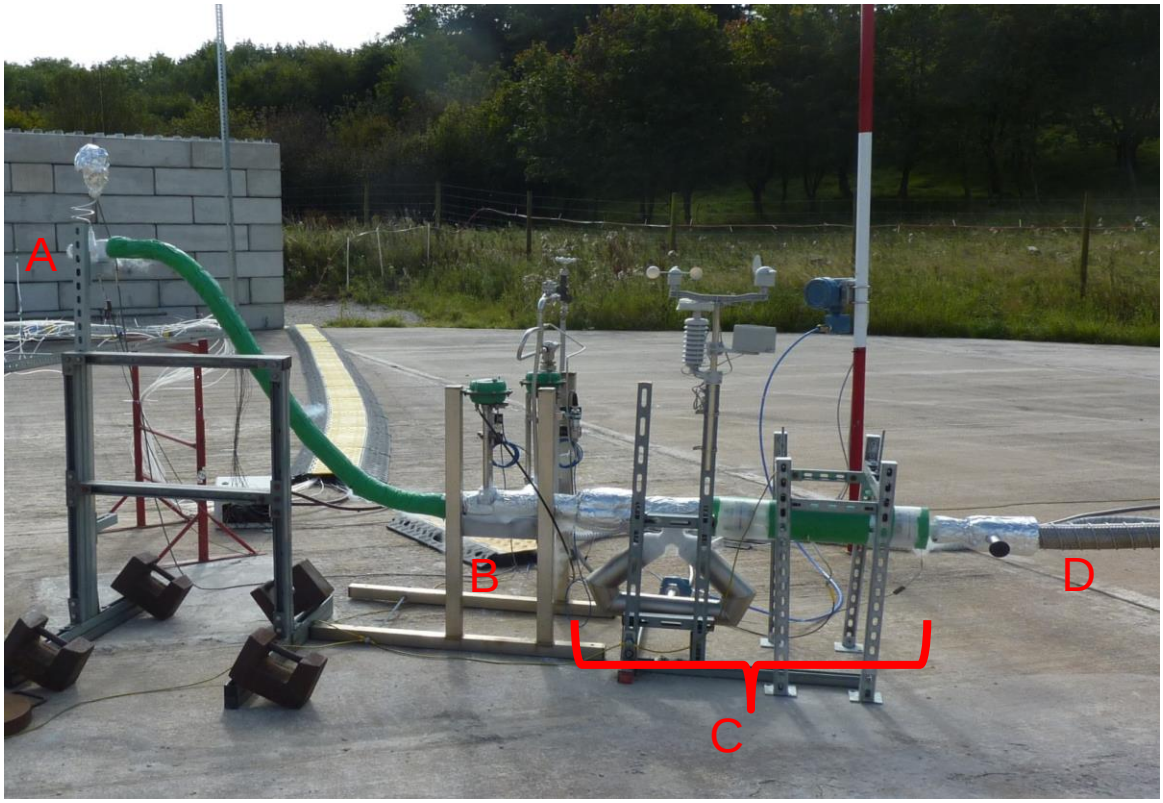

Figure A1: Final section of PRESLHY delivery system

A – Nozzle

B – Final release valve

C – Measurement section (electrostatics and mass flow/density)

D – Vacuum insulated pipe to tanker

7.2 Tests where there was liquid flow up to the nozzle

7.2.1 *5 bar tanker pressure, 12 mm nozzle (Tests 11, 13, 14 and 15)*

Mass flow measurements in all of these tests are broadly consistent at around 265 g/s (Figure A2). This figure, taken with the measured pressure differences across different sections of the pipework, provides a useful indication of the flow resistances. In other tests where the pressure and density are different the flow rate, pressure difference and density are related as $\frac{\dot{M}}{\sqrt{\Delta P.\rho}} = const$ (Eqn 1)

For example, Figure A3 shows the pressure measured before the final release valve. The difference between this and the tanker pressure (plus a small correction for the head of liquid in the tanker) is the pressure difference across the first part of the delivery pipework at the measured flow rate and a density equal to that of liquid hydrogen.

Similarly, the pressure drops across the final section of the pipework and across the nozzle can be derived from the measurements.

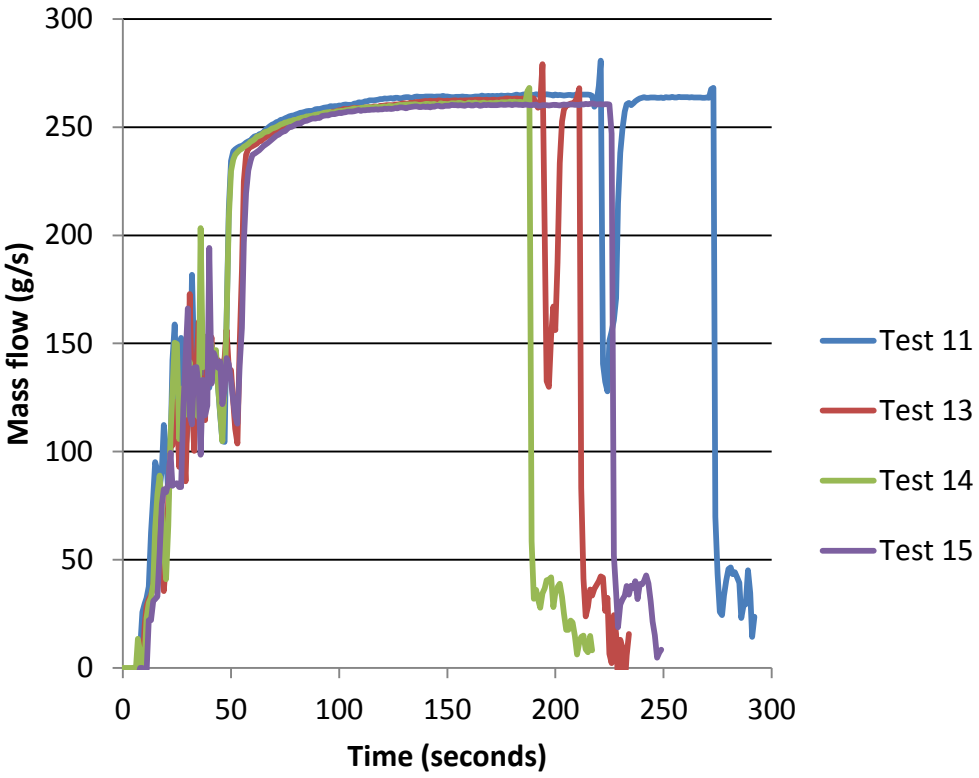

Figure A2: Measured mass flow in Tests 11, 13, 14 and 15

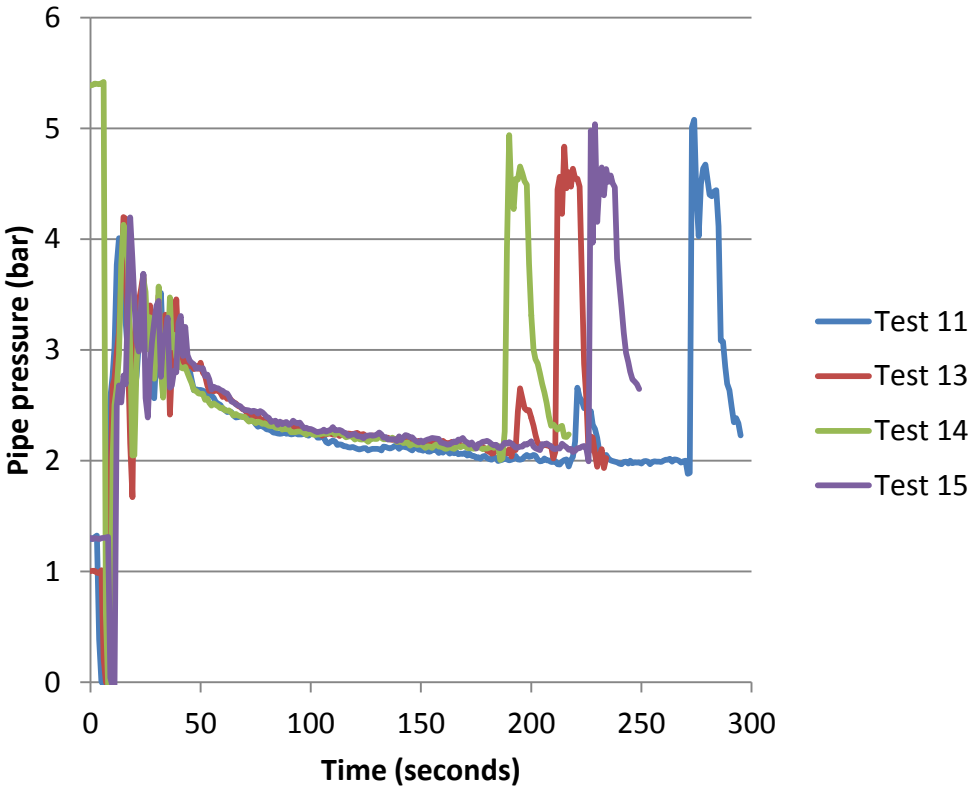

Figure A3: Measured pipe pressure in Tests 11, 13, 14 and 15 (this is the pressure before the final release valve)

The pressure measurement points and derived pressure drops are shown schematically in Figure A4.

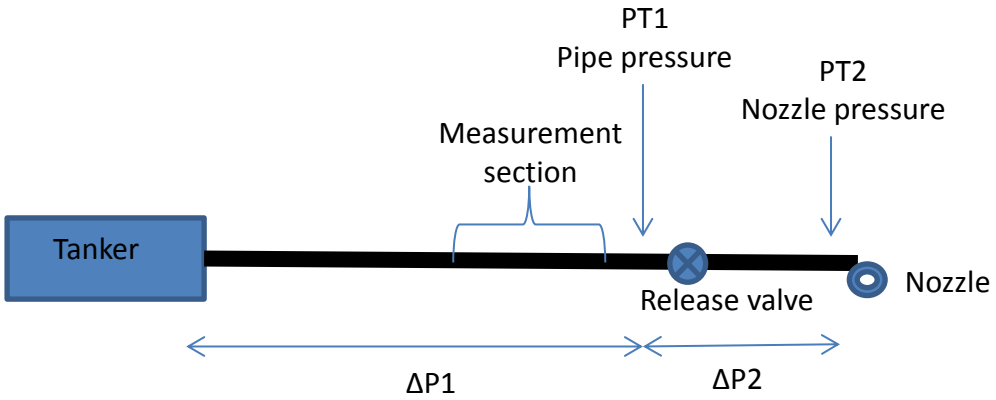

Figure A4: Schematic of measured pressures and derived pressure drops

The approximate pressure drops in various sections of the delivery system for Test 11 are summarised in Table A2. Figures for nozzle and release valve are measured. Emerson provided flow resistance data for the flow meter. The figure for the vacuum hose is estimated from the surface roughness and losses in the tanker are calculated by difference.

Table A2: Pressure drops

Section	**Pressure drop (bar)**
Tanker: Control valves and other fittings	2.6
Vacuum hose and fittings	0.3
Measurement section: mainly flow meter	0.1
Release globe valve	0.34
Nozzle	1.66
Total	5

The ratio of pressure drops ΔP1/ ΔP2 was 8.8 in this case.

The vapour pressure of the released fluid was low (~200 mbar) so the extent of adiabatic flash would have been low (Figure A5) compared with the extent of vaporisation observed in low pressure or open pipe tests. This means that vaporisation was largely a result of heat input to the liquid as it flowed through the delivery system. The distribution of heat input to the liquid follows a very different pattern to the pressure loss shown in Table A2.

Pipework in the tanker and main hose was vacuum insulated and downstream of the flowmeter the pipework was foam insulated. Most of the heat input was in the partially insulated measurement section (Figure A6). Videos of tests also show clouds of condensation coming from this area.

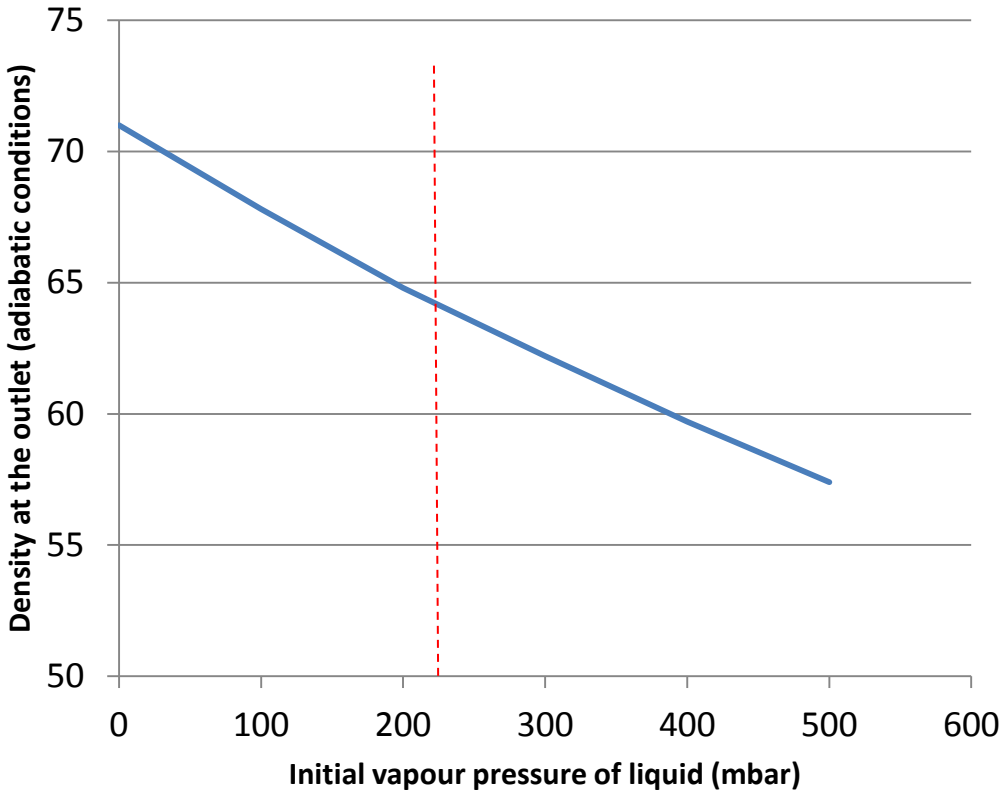

Figure A5: Low levels of density difference driven by adiabatic flash from 200 mbar

Figure A6: Heat losses at flanges in the measurement section and in the flow meter

This distribution of heat input is significant in the analysis of flow rates in other tests where there was 2-phase flow in the flow meter and flow rates have to be derived from pressure measurements. The great majority (97%) of flow resistance of the pipework corresponding to ΔP1 is in the well-insulated section where there would have been no flashing unless the pressure was very low. The measured pressure drop ΔP1 can be used to provide a first estimate of flow rate via Equation 1 and assuming the density of liquid

throughout. The effect of flashing on ΔP1 can be modelled and the results represent a small correction to the derived mass flows. This is described in detail later.

Flow disturbance

Figure A2 and A3 show that in Tests 11 and 13 there were brief (15 second) departures from stable flow. This did not occur in Tests 14 or 15.

Possibly the episodes of disturbed flow corresponded to the detachment of a pocket of vapour somewhere in the delivery system. This would expose the liquid hydrogen flow to a relatively warm section of pipe – that had been insulated by the vapour pocket. When exposed to LH2 the result would have been enhanced heat transfer and some ongoing vapour production for ten seconds or so.

7.2.2 *5 bar tanker pressure, 6 mm nozzle (e.g. Test 12)*

The Emerson flow meter also gave reasonably reliable measurements of mass flow and density with the smaller nozzle. In this case, the reported density (74 kg/m^3) was somewhat closer to the true value of 71 kg/m^3. The mass flow measurements were again apparently disturbed by more frequent detachment of gas bubbles, however, between these episodes a flow rate of 90 - 100 g/s was indicated (Figure A7). The pressure at the nozzle was around 4.5 bar.

The ratio of pressure drops ΔP1/ ΔP2 was also approximately 9 in this case but this could not be measured with the accuracy possible in Test 11 etc. because the low flow corresponds to relatively small pressure drops.

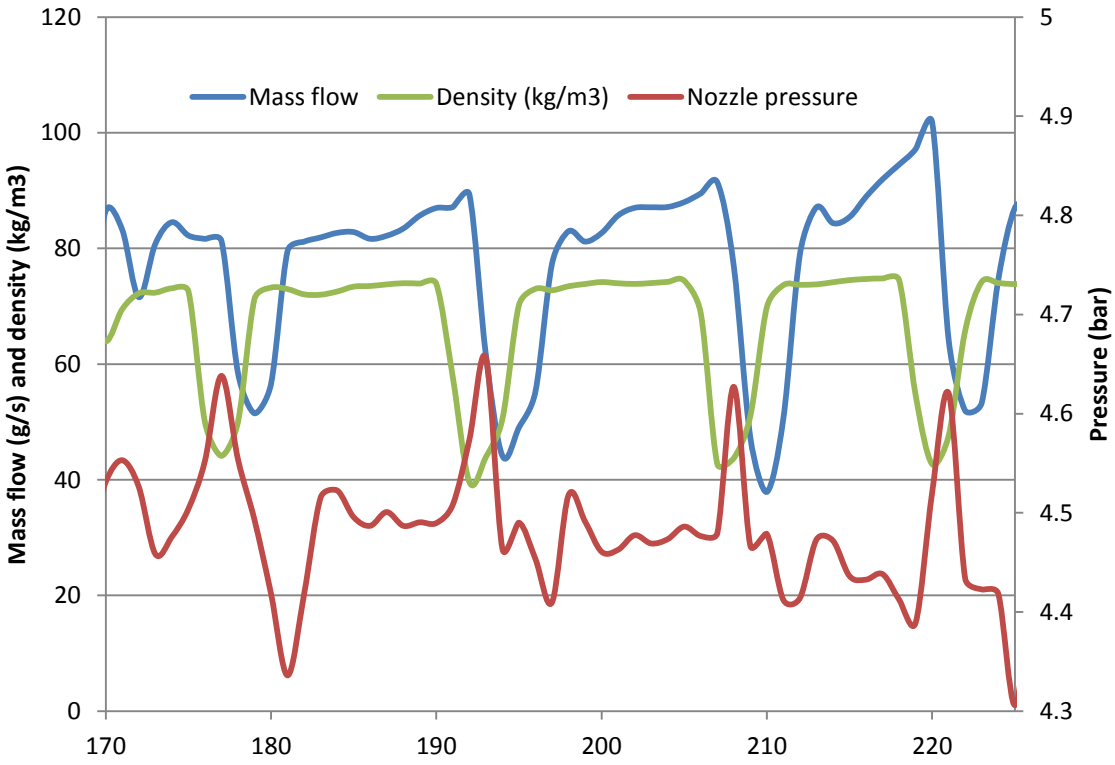

Figure A7: Flow meter and pressure data for part of Test 12

7.3 Tests in which there was flashing prior to the flow meter

7.3.1 *5 bar tanker pressure, 1" nozzle (e.g. Test 10)*

Data from the flow meter and pressure sensors is shown in Figures A8 an A9

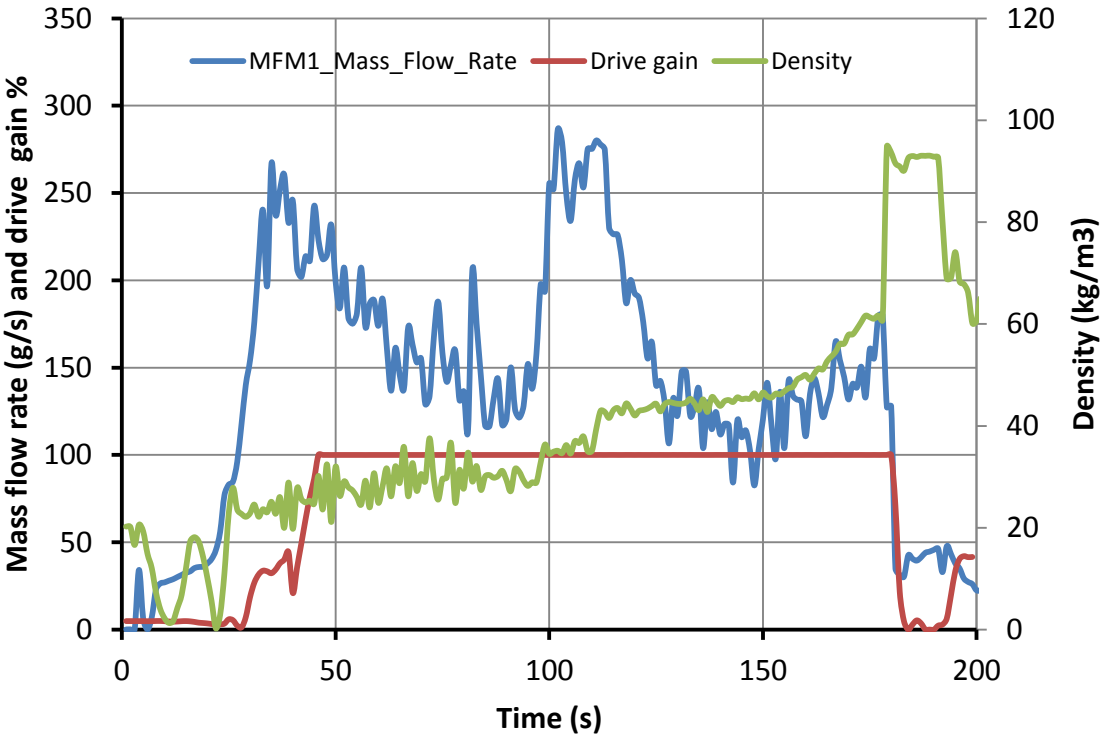

Figure A8: Flow meter data from Test 10 (1" opening, 5 bar pressure)

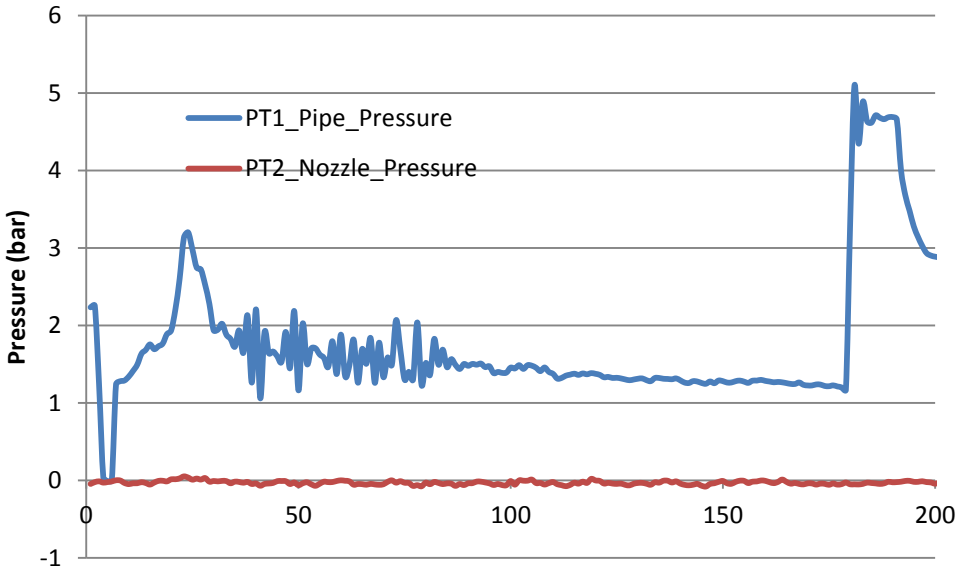

Figure A9: Pressure data from Test 10 (1" opening, 5 bar pressure)

The drive gain[11] is saturated throughout the main release indicating 2-phase flow. However the indicated density gradually increase to around 60 kg/m^3 which is close to the correct value, which suggests the void fraction was quite low i.e. at the flow meter the line pressure was roughly equal to the vapour pressure raised by heat losses.

The gradual changes in pressure and reported density throughout the test suggest that cooling of the pipe with associated vaporisation was not quite complete at the end.

If (as seems very likely in this case) there is little deviation in density in the section of pipe corresponding to ΔP1 – especially at the end of the test - then the flow can be directly related to that in Test 11 via the ratio of the measured pressure drops.

Test 11: ΔP1 = 3.0 bar

Test 10: ΔP1 = 3.8 bar

The ratio of the mass flow rates is $\sqrt{\frac{3.8}{3}} = 1.125$

Since the mass flow rate in Test 11 was 265 g/s this means the rate in Test 10 was about 298 g/s.

It seems reasonable that some increase in flow results from removing the ½" nozzle – but that the effect is fairly small as it allows earlier flashing - in the pipe rather than at the nozzle.

7.3.2 *1 bar tanker pressure, ½" nozzle (e.g. Test 4)*

In tests with lower (1 bar) tanker pressure the flow into the flow meter had a high void fraction (pressure measurement indicate this was typically of order 80%). Decoupling between the gas and liquid phases means that the mass flow meter cannot work in such circumstances and the mass flow is grossly underestimated. Figure A10 shows a mass flow of around 15 g/s whereas the true figure is over 100 g/s.

In this case, we have to rely on pressure measurements to determine flow.

In Test 4

ΔP1 = 0.475 bar (48%) ΔP2= 0.152 bar (15.3%) Across nozzle = 0.362 bar (36.5%)

This can be compared with the equivalent 5 bar test (Test 11)

ΔP1 = 3 bar (60%) ΔP2= 0.34 bar (6.8%) Across nozzle = 1.66 bar (33%)

As the tanker pressure is lowered, there is a substantial increase in the pressure drop across the final section of the pipe (before the nozzle). Presumably, this is because the flow is flashing here whereas at high pressure it was not. The ratio of pressure drops ΔP1/ ΔP2 was 3.2 in this case (compared with 8.8 for an all-liquid flow).

The proportion of the total pressure across the nozzle does not change much. Presumably, this is because even at higher tank pressure, there would have been some flashing at the nozzle and the density would already have been well below that of liquid at the vena contracta.

[11] Drive gain is recorded by the mass flow meter – it indicates the power expended in attempting to maintain stable vibrations conditions and is consequently an indicator of the phase variability of the flow.

To be able to interpret these measurements further and correct for the vaporisation in the last part of the pipework corresponding to ΔP2 requires an approximate analysis of pressure loss and heat input to the liquid in the supply system

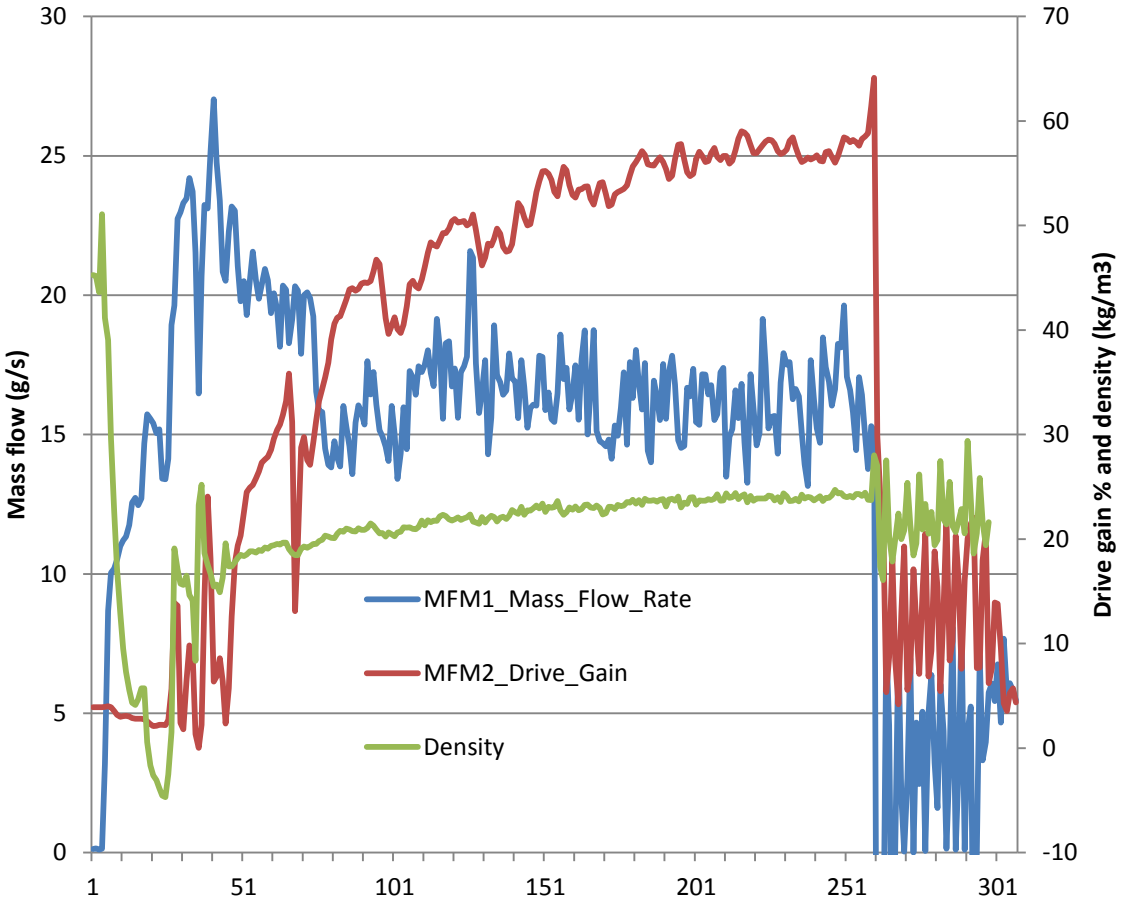

Figure A10: Flow meter measurements in Test 4

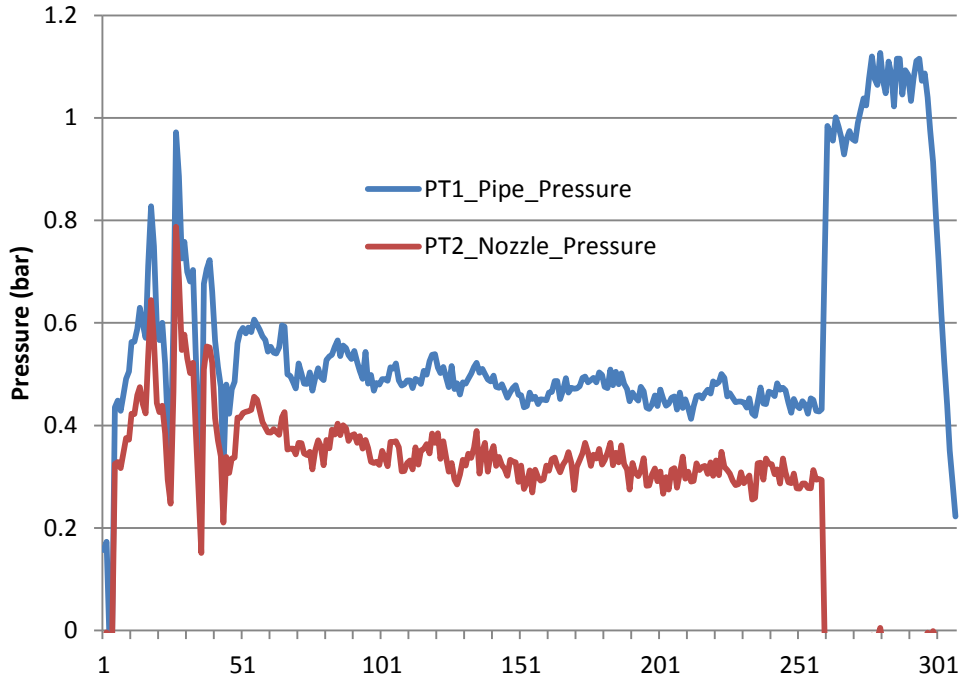

Figure A11: Flow meter measurements in Test 4

7.3.3 *Modelling*

Almost all of the flashing is as a result of heat transfer into the liquid flow and most of this occurs in the uninsulated parts of the measurement section.

If the pipe pressure is high the effects of this heat transfer may not appear as vapour production until the flow depressurises closer to the nozzle (5 bar tests). In lower pressure cases, heat transfer causes immediate vaporisation.

In the latter cases, it is no longer comfortable to assume liquid densities throughout the ΔP1 section. Instead, assume that flashing occurs at the start of the measurement section and that the density decreases by a factor of X then remains constant through the rest of the pipe.

If the proportion of flow resistance in the ΔP1 section that is associated with the measurement section is F then the measured ratio $\frac{\Delta P_1}{\Delta P_2}$ is related to X and F as

$$X = \frac{8.8\ (1-F)}{\frac{\Delta P_1}{\Delta P_2} - 8.8F}$$ (8.8 is the ratio $\frac{\Delta P_1}{\Delta P_2}$ when there is no change in density)

The simple model leading to this prediction is illustrated in Figure A12.

The data in Table A2 suggest F is approximately 3%. A number of values around this figure have been used to indicate sensitivity of the derived density reduction factors and flow rates to the assumptions made.

For example in Test 4:

If F = 0%, $\frac{\Delta P_1}{\Delta P_2}$=3.2 then X = 2.75 i.e. $\frac{\rho 2}{\rho 1}$ = 1 / 2.75 = 0.36

If F = 3%, $\frac{\Delta P_1}{\Delta P_2}$=3.2 then X = 2.9 i.e. $\frac{\rho 2}{\rho 1}$ = 1 / 2.9 = 0.34

If F = 6%, $\frac{\Delta P_1}{\Delta P_2}$=3.2 then X = 3.1 i.e. $\frac{\rho 2}{\rho 1}$= 1 / 3.1 = 0.32

Because of flashing in the measurement section the effective flow resistance (to liquid flow) of the pipework corresponding to ΔP1 increases by a factor k where

k = 1 + (X-1).F

Results of this type of analysis for the low-pressure tests are shown in Table A3.

The mass flow rates are calculated from the pressure drop for (all liquid flow) at 5 bar using the effective resistance coefficients k and measured pressure drops in respective tests

$$Flow \propto \sqrt{\frac{\Delta P}{k}}$$

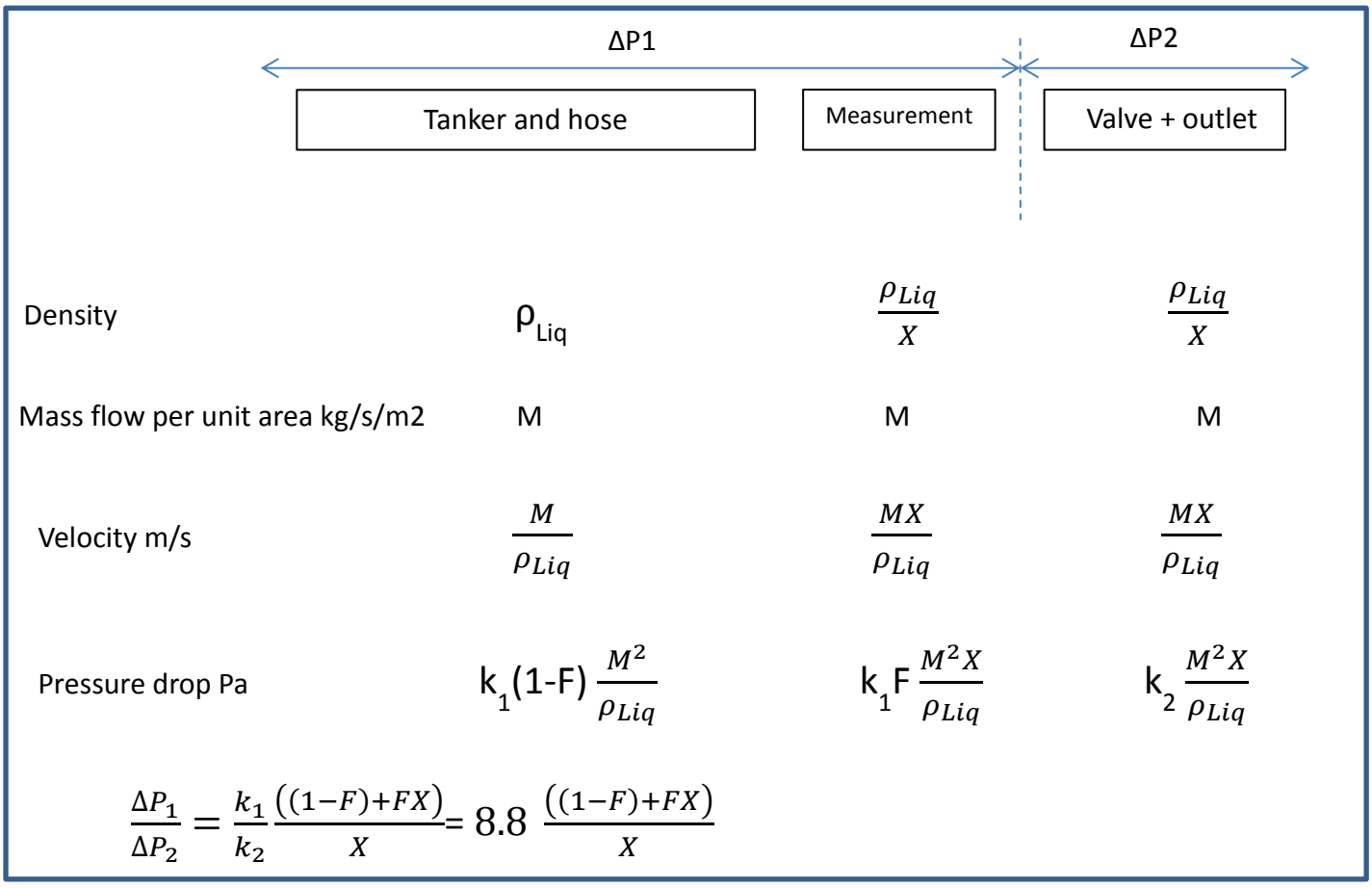

Figure A12: Simple model of vaporisation and pressure loss

(8.8 is the ratio $\frac{\Delta P_1}{\Delta P_2}$ when there is no change in density)

Table A3: Results of flow rate analysis

	Pressure drop ΔP1 (measured) bar	**Density reduction factor X**	**Relative Flow resistance - over ΔP1 k**	**Flow (g/s)**
Test 11 (5 bar, ½" nozzle, liq)	2.91	1	1	265
Test 4 (1 bar, ½" nozzle) F = 0 F = 3 % F = 6 %	 0.475 0.475 0.475	 2.75 2.9 3.1	 1 1.06 1.13	 107 104 101
Test 3 or 16 (1 bar, open pipe) F = 0 F = 3 % F = 6 %	 0.86 0.86 0.86	 2.85 3.0 3.2	 1 1.06 1.13	 144 140 135

It seems sensible that the flow through an open pipe (135-144 g/s) is somewhat greater than when there is a ½" nozzle (101-107 g/s).

It also seems reasonable that the ratio of these flow rates (which is 1.34) is a little more than the ratio for the 5 bar tanker pressure case 298/265 = 1.125, since in the 5 bar case the ½" nozzle prevents flashing (in the pipe) altogether.

7.4 Heat transfer and vapour pressure

It is interesting to consider the energy input level implied by these estimates of density reduction.

A value of X (density reduction) implies a fractional vaporisation rate of:

$$\frac{M_g}{M_L} = \frac{\rho_g}{\rho_L} \cdot \left(\frac{X-1}{1 - \frac{\rho_g}{\rho_L} X} \right)$$

The gas density and therefore the relationship between density ratio and vaporisation is a function of pressure (Figure A13).

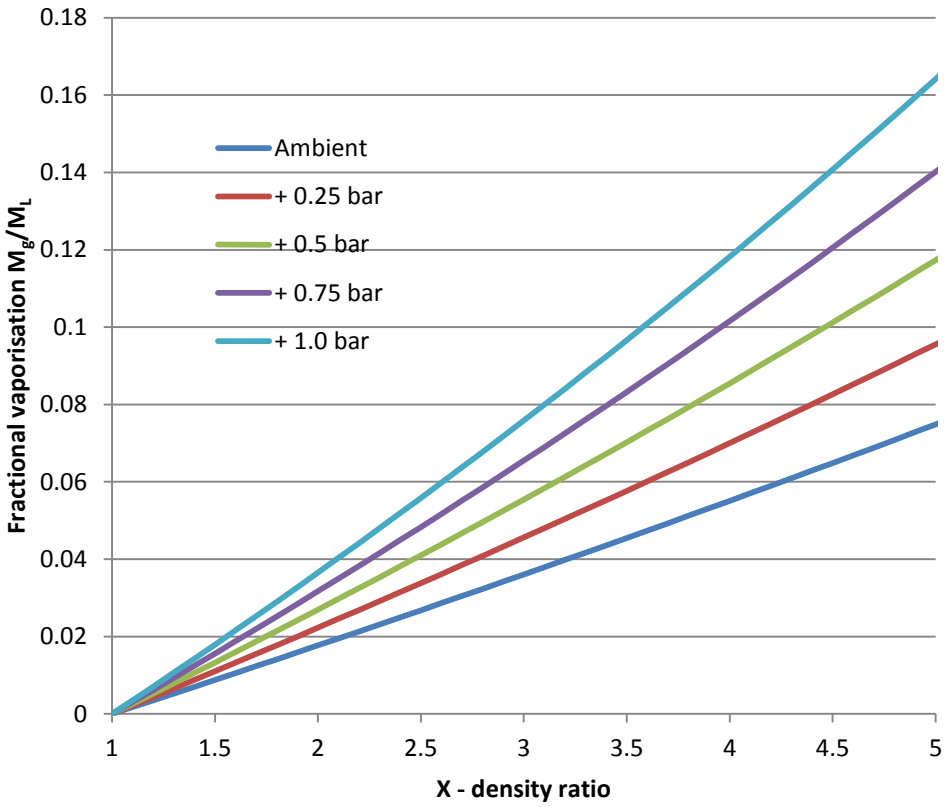

Figure A13: Relationship between observed density ratio and fractional vaporisation rate

At 0.5 bar (over ambient) a density ratio of 3 (see Table A3) implies a vaporisation rate of about 5.5%.

At 1.0 bar a density ratio of 3 implies a vaporisation rate of about 7.5%.

The heat of vaporisation is around 900 J/mole, so these levels of vaporisation imply a heat input of 50 – 67.5 J/mol (if the pressure was between 0.5 and 1 bar over ambient).

If the initial vapour pressure was 200 mbar then inputs of 50 – 67.5 kJ /mole would have raised the saturation over-pressure to between 1.2 and 1.5 bar (Figure A14).

We do not have useful equivalent data for the smallest (6mm) nozzle. It seems likely that the longer transit times through the measuring section would have led to somewhat higher values of heat transfer and final vapour pressure i.e. final value >1.5 bar.

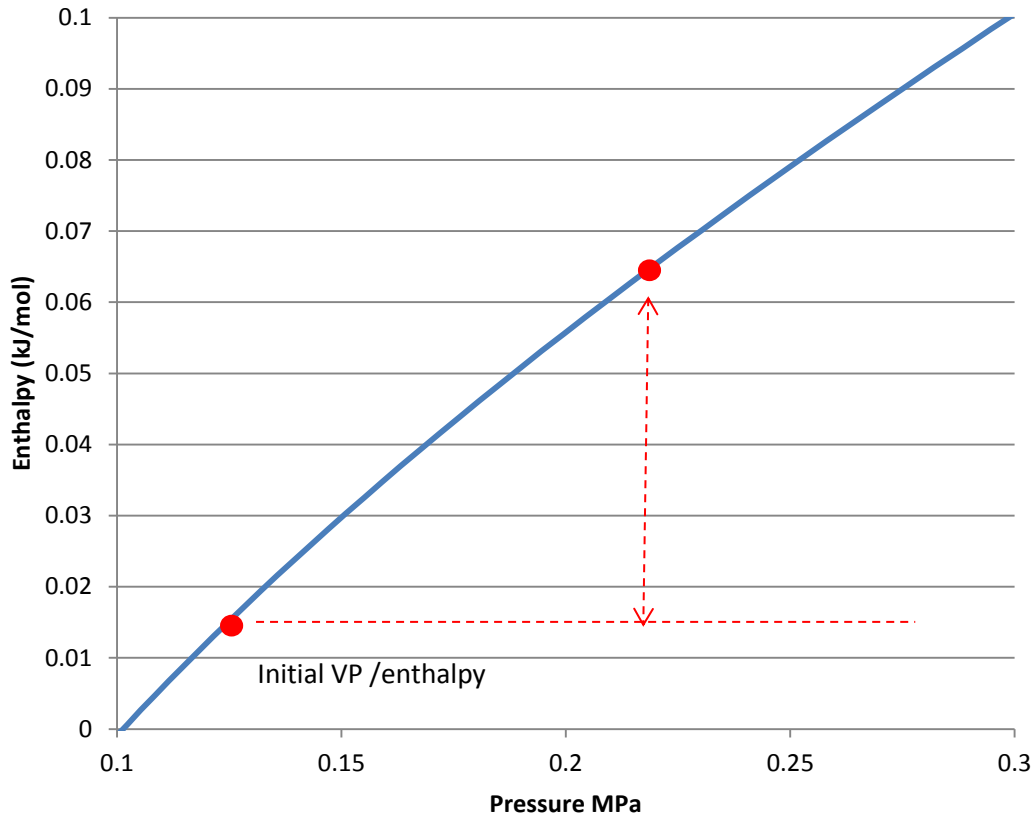

Figure A14: Increase in vapour pressure caused by energy input of 50 J/mol

This analysis broadly explains the phase composition at the flow meter and the consequent variation in effectiveness of the device (Table A4).

Table A4: Phase composition at the flow meter

Tanker Pressure	Nozzle size	Approx measured pressure at flow meter (bar)	Expected vapour pressure (bar)	Expected phase at meter	Observed phase at meter
5 bar	6mm (¼ ”)	4.5	>1.5	liquid	liquid
5 bar	12mm (½”)	2	1.2 - 1.5	liquid	liquid
5 bar	1”	1.2	1.2 - 1.5	Marginal (small gas content)	Marginal (small gas content)
1 bar	6mm (¼ ”)	<1	>1.5	Gassy	Gassy
1 bar	12mm (½”)	0.5	1.2-1.5	Gassy	Gassy
1 bar	1”	0.2	1.2-1.5	Gassy	Gassy

7.5 Flow rates in previous tests series using Liquid Hydrogen

Previous work (HSE Research Reports RR987 and RR986) used a very similar set up but without the measurement section. The releases were of “flattened” hydrogen from a tanker with the vapour space re-pressurised to 1 bar. There was no restriction on the outlet. The valve and final hose to the end of the pipe were not insulated (Figure A15).

Figure A15: Previous release configuration

The flow resistance coefficient in the stages prior to the valve would have been less than PRESLHY by a factor of 1-F, because of the missing measurement section. It seems reasonable to assume that little if any flashing occurred in this section.

There would have been rapid flashing in the valve and final delivery pipe. Density reduction factors in a similar range to those observed in the equivalent PRESLHY tests might have been expected.

In the RR986 set up the proportion of tanker pressure up to the valve, relative to the total pressure drop, is:

$$\frac{8.8(1-F)}{8.8(1-F)+X}$$

The effective flow resistance up to the valve (relative to the equivalent PRESLHY test) is also reduced by a factor of 1-F.

Comparing the pressure drop and flow resistance with the values in Test 11 the flow rate in previous work can be calculated using the relationship:

$$Flow \propto \sqrt{\frac{\Delta P}{k}}$$

Assuming a density reduction factor of 3 gives an estimate of about 135 g/s for the mass flow rate in the previous work (Table A5).

The density reduction factor for the uninsulated outlet pipe is not known. Assumed values of X=1.5 and 6 would lead to estimates of flow of 145 g/s and 121 g/s respectively. It is likely the flow was somewhere in the range 120 - 150 g/s.

Table A5: Flow rates in PRESLHY and previous tests

	Pressure drop ΔP1 bar	Density reduction factor X	Relative Flow resistance - over ΔP1 k	Flow (g/s)
Test 11 (5 bar , ½" nozzle)	Measured 2.91	1	1	265
Test 3 or 16 (1 bar, open pipe)				
F = 0	0.86	2.85	1	144
F = 3 %	0.86	3.0	1.06	140
F = 6 %	0.86	3.2	1.13	135
RR 986 (1 bar, open pipe)	Calculated	Assumed		
F=0	0.745	3	1	134
F=3%	0.74	3	0.97	136
F=6%	0.733	3	0.94	137

8 Appendix 2: Formation of solids during mixing of LH2 and air

Mass of LH2 (kg)	35.1	35.1	35.1	35.1
Air Temp (K)	288	288	288	288
Final temperature (K)	20	58	20	52
Oxygen compostion solid %	21	21	44	44
Fraction of air condensed	1	1	0.3	0.3
ΔH Cooling to 68 K (kJ/mol)	6.82	6.82	6.82	6.82
ΔH Condensation (kJ/mol)	5.85	5.85	1.755	1.755
ΔH Freezing (kJ/mol)	0.58	0.58	0.174	0.174
Cooling to final temp (kJ/mol)	2.16	0.45	0.648	0.216
ΔH Total (kJ/mol)	15.41	13.7	9.397	8.965
ΔH H2 Vap (kJ/mol)	0.9	0.9	0.9	0.9
ΔH H2 warming (kJ/mol)	0	0.8132	0	0.6848
Total (kJ/mol)	0.9	1.7132	0.9	1.5848
Mole ratio: LH2 vaporised/air	17.12	8.00	34.80	18.86
Mass ratio (LH2/solid air)	1.19	0.55	2.34	1.27
Mass of solid air	29.56	63.29	15.01	27.70
Mass of oxygen	6.89	14.75	7.10	13.10